

National Park Service  
U.S. Department of the Interior

Northeast Region  
Boston, Massachusetts



## **Evaluation of Marsh Development Processes at Fire Island National Seashore (New York): Recent and Historic Perspectives**

Technical Report NPS/NER/NRTR – 2007/089



**ON THE COVER**

Sampling salt marsh elevation using a Surface Elevation Table (photograph courtesy of Charles Roman)

---

# **Evaluation of Marsh Development Processes at Fire Island National Seashore (New York): Recent and Historic Perspectives**

Technical Report NPS/NER/NRTR – 2007/089

CHARLES T. ROMAN  
National Park Service  
North Atlantic Coast Cooperative Ecosystem Studies Unit  
University of Rhode Island  
Narragansett, RI 02882  
charles\_roman@nps.gov

JOHN W. KING  
Graduate School of Oceanography  
University of Rhode Island  
Narragansett, RI 02882  
jking@gso.uri.edu

DONALD R. CAHOON and JAMES C. LYNCH  
USGS Patuxent Wildlife Research Center  
10300 Baltimore Ave., BARC-East Bldg #308  
Beltsville, MD 20705  
don\_cahoon@usgs.gov  
jclynch@usgs.gov

PETER G. APPLEBY  
Department of Mathematical Sciences  
Room 425, M&O Building  
University of Liverpool  
Liverpool L69 3BX, UK  
appleby@liverpool.ac.uk

July 2007

U.S. Department of the Interior  
National Park Service  
Northeast Region  
Boston, Massachusetts

The Northeast Region of the National Park Service (NPS) comprises national parks and related areas in 13 New England and Mid-Atlantic states. The diversity of parks and their resources are reflected in their designations as national parks, seashores, historic sites, recreation areas, military parks, memorials, and rivers and trails. Biological, physical, and social science research results, natural resource inventory and monitoring data, scientific literature reviews, bibliographies, and proceedings of technical workshops and conferences related to these park units are disseminated through the NPS/NER Technical Report (NRTR) and Natural Resources Report (NRR) series. The reports are a continuation of series with previous acronyms of NPS/PHSO, NPS/MAR, NPS/BSO-RNR and NPS/NERBOST. Individual parks may also disseminate information through their own report series.

Natural Resources Reports are the designated medium for information on technologies and resource management methods; "how to" resource management papers; proceedings of resource management workshops or conferences; and natural resource program descriptions and resource action plans.

Technical Reports are the designated medium for initially disseminating data and results of biological, physical, and social science research that addresses natural resource management issues; natural resource inventories and monitoring activities; scientific literature reviews; bibliographies; and peer-reviewed proceedings of technical workshops, conferences, or symposia.

Mention of trade names or commercial products does not constitute endorsement or recommendation for use by the National Park Service.

This report was accomplished under Cooperative Agreement 1443CA4520-99-007, task agreement J4525037D38 (University of Rhode Island) and Interagency Agreement 1443-F4520-02-0018 with the USGS, with assistance from the NPS. The statements, findings, conclusions, recommendations, and data in this report are solely those of the author(s), and do not necessarily reflect the views of the U.S. Department of the Interior, National Park Service.

Print copies of reports in these series, produced in limited quantity and only available as long as the supply lasts, or preferably, file copies on CD, may be obtained by sending a request to the address on the back cover. Print copies also may be requested from the NPS Technical Information Center (TIC), Denver Service Center, PO Box 25287, Denver, CO 80225-0287. A copy charge may be involved. To order from TIC, refer to document D-129.

This report may also be available as a downloadable portable document format file from the Internet at <http://www.nps.gov/nero/science/>.

Please cite this publication as:

Roman, C.T., J.W. King, D.R. Cahoon, J.C. Lynch, and P.G. Appleby. July 2007. Evaluation of marsh development processes at Fire Island National Seashore (New York): recent and historic perspectives. Technical Report NPS/NER/NRTR – 2007/089. National Park Service, Boston, MA.

## ABSTRACT

Salt marshes are dynamic environments, increasing in vertical elevation and migrating, often landward, as sea level rises. With sea level rise greater than marsh elevation increase, marshes can be submerged, marsh soils become waterlogged, and plant growth becomes stressed, often resulting in conversion of vegetation-dominated marsh to mudflat or open water habitat. Given that the rate of sea level rise is expected to accelerate over the next century, it is important to understand the processes that control marsh development. More specifically, the objectives of this project were to quantify vertical marsh elevation change in relation to recent rates of sea-level rise and to investigate factors or processes that are most influential in controlling the development and maintenance of Fire Island salt marshes.

The 50-km Fire Island is located on the south shore of Long Island (NY). The island is bordered by Moriches Inlet to the east and Fire Island Inlet to the west, exchanging with the Atlantic Ocean and the back-barrier lagoon system of Great South Bay and Moriches Bay. *Spartina alterniflora* dominated salt marsh occurs along the bay shoreline of Fire Island. Three marsh areas were selected for study; Great Gun Meadows, Hospital Point, and Watch Hill, 2.5 km, 12 km, and 20 km, respectively, from Moriches Inlet.

Surface Elevation Tables (SETs), in conjunction with feldspar marker horizons, were used to evaluate recent (2002 to 2007) relationships between marsh surface elevation change and rates of relative sea level rise and understand the surface and subsurface processes that influence marsh elevation change. The elevation of a salt marsh is controlled by sediment accretion and organic matter build-up, resulting in increases in elevation, while the subsurface processes of sediment compaction/subsidence and organic matter decomposition, as well as erosion of surface sediments contribute to elevation loss. The surface accretionary processes are monitored by repeated sampling of artificial marker horizon plots and marsh surface elevation is correspondingly monitored with the surface elevation table. SETs and marker horizons were established at the three marsh areas in August 2002, with monitoring proceeding for a 58 month period to May 2007. SET and marker horizon monitoring is planned to continue for the long-term. Marsh surface elevation change is compared to sea level rise to determine if the marsh is keeping pace with sea level.

All three sites reveal an elevation deficit when compared to sea level rise; the marshes appear to not be keeping pace with rates of sea level rise. Based on the SET elevation monitoring during the 58 month study period, elevation change of the marsh surface ranged from an increase of 2.04 mm y<sup>-1</sup> and 2.08 mm y<sup>-1</sup> at Hospital Point and Watch Hill, respectively, to an elevation decline of -1.05 mm y<sup>-1</sup> at Great Gun. Records of relative sea level over the past 60 to 100 years from NOAA water level stations in the vicinity of Great South Bay/Moriches Bay (Montauk Point and Battery, NY; Sandy Hook, NJ) ranged from 2.52 mm y<sup>-1</sup> to 3.79 mm y<sup>-1</sup>, all greater than measured marsh elevation changes. However, it is noted that the marsh surface elevation trend determined for Great Gun may not be representative of the larger Great Gun marsh because the SET

monitoring may have occurred in a portion of marsh where a natural marsh drainage was forming.

At each site vertical accretion (measured by the feldspar marker horizons) was greater than the marsh surface elevation change at all sites. Sediment accumulated on the marsh surface (vertical accretion), but the elevation of the marsh surface did not reflect this accumulation, suggesting shallow subsidence (surface accretion is greater than elevation gain). Shallow subsidence suggests that subsurface processes such as autocompaction of marsh sediments, decomposition of belowground organic matter, and changes in belowground water storage are likely all contributing to the observed elevation deficit.

To evaluate longer-term or historic trends (decades to centuries) in marsh development processes at Fire Island, sediment cores approximately 1-m deep, were collected from the three marsh areas. Stratigraphy of the cores was evaluated by digital imagery and measures of magnetic susceptibility, wet bulk density, and organic content by loss-on-ignition. Radiometric dating of the cores was accomplished by  $^{210}\text{Pb}$  and  $^{137}\text{Cs}$ .

Based on the chronology from radiometric dating of the cores, it was estimated that salt marsh development was initiated at the Great Gun site around 1766 AD and Hospital Point near 1778, coinciding with establishment of nearby Halletts (1788) and Smiths (1773) inlets, respectively. The role of storm-induced inlets and barrier island overwash events in the bayward transport of sediment, flood tidal delta formation, and marsh development is well-known. Also related to inlets, at the Great Gun marsh there was a clear correlation between the opening of Moriches Inlet in 1931 and the abrupt termination of salt marsh peat development, replaced by deposition of inorganic sediment. It is likely that the tidal range increased substantially at Great Gun with the opening of the new inlet, the existing *Spartina* marsh was inundated and converted to tidal flat, then with subsequent re-development of marsh to the present as hydrologic conditions became favourable for vegetation to thrive. Inlets and associated flood tidal deltas represent a fundamental process supporting the establishment of back-barrier salt marsh habitat. The long-term maintenance of salt marshes at Fire Island seems tightly coupled to preservation of inlet processes.

The Fire Island marsh study sites are in an elevation deficit relative to the long-term rate of sea-level rise at Sandy Hook. This deficit trend could continue for the long-term, there could be a pulse of sediment delivered to the marsh surface during a future storm event, or the marshes may have the capacity to periodically adjust, over the long-term, during episodes of low rates of sea-level rise. If the observed elevation deficit continues, it is likely that the Fire Island marshes will become wetter, areas of high marsh *Spartina patens* may convert to *Spartina alterniflora*, and open water habitat may increase. There could also be a landward encroachment of marshes to upland areas, a natural process of marsh development in response to sea level rise, assuming that cultural development (e.g., bulkheads) will not impede this migration. Given that the global rate of sea-level rise is expected to accelerate over the next century, and that some marshes in the northeast show evidence of submergence, it is especially important to continue monitoring of marsh elevation changes in response to sea-level rise.

# TABLE OF CONTENTS

|   |      |
|---|------|
| <b>ABSTRACT</b> .....   | iii  |
| <b>TABLE OF CONTENTS</b> .....  | v    |
| <b>LIST OF FIGURES</b> .....  | vi   |
| <b>LIST OF TABLES</b> .....   | vii  |
| <b>ACKNOWLEDGEMENTS</b> .....   | viii |
| <br>  |      |
| <b>CHAPTER 1: Purpose of Study and Description of Study Site</b> .....          | 1    |
| INTRODUCTION AND PROBLEM STATEMENT .....  | 1    |
| STUDY SITE .....  | 2    |
| LITERATURE CITED .....  | 3    |
| <br>  |      |
| <b>CHAPTER 2: Monitoring Marsh Surface Elevation Change</b> .....               | 9    |
| INTRODUCTION TO SET AND MARKER HORIZON METHOD .....                             | 9    |
| METHODS .....   | 10   |
| RESULTS AND DISCUSSION .....  | 11   |
| Marsh Elevation, Vertical Accretion, Shallow Subsidence .....                   | 11   |
| Relation of marsh surface elevation to sea level rise .....                     | 12   |
| Relation of marsh surface elevation to sea level rise: Comments for Great Gun . | 14   |
| Marsh elevation change and vertical accretion variation among sites .....       | 14   |
| Long-term monitoring and marsh development processes .....                      | 15   |
| LITERATURE CITED .....  | 15   |
| <br>  |      |
| <b>CHAPTER 3: Radiometric Dating and Analysis of Marsh Sediment Cores</b> ..... | 27   |
| INTRODUCTION .....  | 27   |
| METHODS .....   | 27   |
| RESULTS .....   | 28   |
| Core Logging and Lithology .....  | 28   |
| Radiometric Dating .....  | 29   |
| Timing of Changes in Organic Content .....                                      | 32   |
| DISCUSSION .....  | 32   |
| Initiation of Peat Deposition .....   | 32   |
| Impact of Storms and Inlet Changes .....  | 32   |
| Comparison of Accretion Rates .....   | 33   |
| LITERATURE CITED .....  | 33   |
| <br>  |      |
| <b>CHAPTER 4: Summary of Findings and Management Implications</b> .....         | 59   |
| PURPOSE AND SIGNIFICANCE OF STUDY .....   | 59   |
| STUDY SITE AND METHODS: A REVIEW .....  | 59   |
| FINDINGS: RECENT TRENDS IN MARSH DEVELOPMENT PROCESSES ....                     | 60   |
| FINDINGS: HISTORIC TRENDS, THE ROLE OF INLETS .....                             | 61   |
| RESOURCE MANAGEMENT IMPLICATIONS AND RESEARCH NEEDS ....                        | 61   |
| LITERATURE CITED .....  | 62   |

## LIST OF FIGURES

|      |  |    |
|------|--|----|
| 1.1  | Regional location of study marshes .....   | 6  |
| 1.2  | Mean and spring tide range .....   | 7  |
| 1.3  | Location of historic inlets .....  | 8  |
| 2.1  | Schematic and photographs of SET and marker horizon method .....                     | 19 |
| 2.2  | Aerial view of three study sites and SET locations .....                             | 20 |
| 2.3  | Marsh surface elevation change and vertical accretion, 3 sites .....                 | 21 |
| 2.4  | Mean annual sea level at Sandy Hook, NJ .....  | 22 |
| 2.5  | Marsh surface elevation, individual replicate SETs .....                             | 23 |
| 3.1  | Location of core collection sites .....  | 35 |
| 3.2  | Core log and digital image, Watch Hill core 3-1 .....                                | 36 |
| 3.3  | Core log and digital image, Watch Hill core 3-2 .....                                | 37 |
| 3.4  | Core log and digital image, Watch Hill core 3-3 .....                                | 38 |
| 3.5  | Core log and digital image, Hospital Point core 2-1 .....                            | 39 |
| 3.6  | Core log and digital image, Hospital Point core 2-2 .....                            | 40 |
| 3.7  | Core log and digital image, Hospital Point core 2-3 .....                            | 41 |
| 3.8  | Core log and digital image, Great Gun core 1-1 .....                                 | 42 |
| 3.9  | Core log and digital image, Great Gun core 1-2 .....                                 | 43 |
| 3.10 | Core log and digital image, Great Gun core 1-3 .....                                 | 44 |
| 3.11 | Organic content, Watch Hill core 3-2 .....   | 45 |
| 3.12 | Organic content, Hospital Point core 2-1 .....                                       | 46 |
| 3.13 | Organic content, Great Gun core 1-2 .....  | 47 |
| 3.14 | $^{210}\text{Pb}$ and $^{137}\text{Cs}$ core profiles, Great Gun core 1-2 .....      | 48 |
| 3.15 | Radiometric chronology, Great Gun core 1-2 .....                                     | 49 |
| 3.16 | $^{210}\text{Pb}$ and $^{137}\text{Cs}$ core profiles, Hospital Point core 2-1 ..... | 50 |
| 3.17 | Radiometric chronology, Hospital Point core 2-1 .....                                | 51 |
| 3.18 | $^{210}\text{Pb}$ and $^{137}\text{Cs}$ core profiles, Watch Hill core 3-2 .....     | 52 |
| 3.19 | Radiometric chronology, Watch Hill core 3-2 .....                                    | 52 |
| 3.20 | Percent organic carbon vs. calendar year, 3 sites .....                              | 53 |



## LIST OF TABLES

|     |  |    |
|-----|--|----|
| 2.1 | UTM site coordinates, depth of SET benchmark, area vegetation type .....       | 24 |
| 2.2 | Marsh surface elevation change and vertical accretion rate, 3 sites.....       | 25 |
| 2.3 | Rate of sea level rise from NY\NJ area NOAA water level stations .....         | 26 |
| 3.1 | Radionuclide concentrations, Great Gun core 1-2 .....                          | 54 |
| 3.2 | Radionuclide concentrations, Hospital Point core 2-1 .....                     | 55 |
| 3.3 | Radionuclide concentrations, Watch Hill core 3-2 .....                         | 55 |
| 3.4 | Radionuclide parameters, 3 cores .....   | 56 |
| 3.5 | <sup>210</sup> Pb chronology and sedimentation rates, Great Gun 1-2 .....      | 56 |
| 3.6 | <sup>210</sup> Pb chronology and sedimentation rates, Hospital Point 2-1 ..... | 57 |
| 3.7 | <sup>210</sup> Pb chronology and sedimentation rates, Watch Hill 3-2 .....     | 57 |
| 3.8 | Mean post-1963 sedimentation rate, 3 sites .....                               | 58 |
| 3.9 | Comparison of marsh accretion rates using three methods .....                  | 58 |

## ACKNOWLEDGEMENTS

Thanks are extended to Fire Island National Seashore for providing boats and boat maintenance and providing field personnel for assistance with sampling. In addition to the extensive assistance provided by Fire Island National Seashore permanent and seasonal staffs, personnel from the USGS Patuxent Wildlife Research Center and University of Rhode Island students were instrumental during all phases of the field work, including establishment of the SET benchmark pipes, SET data collection, and core collection. Special thanks are extended to Michael Bilecki, Marie Lawrence, Daniel Barrera and Fernando Villalba of the Fire Island National Seashore Natural Resources Division and Patti Rafferty (NPS, NE Region) for local logistical support throughout the study. Mary-Jane James-Pirri (University of Rhode Island) and Philippe Hensel (USGS) are gratefully acknowledged for their assistance with statistical analysis of the SET data. Carol Gibson and Danielle Cares (University of Rhode Island) are thanked for their involvement in all aspects of the sediment core study, including laboratory analysis, data analysis, and report preparation.

Acknowledgement goes to Norbert Psuty (Rutgers University) and two anonymous reviewers for their comments on a draft of this final report.

Smith Point County Park (Suffolk County Parks) officials provided access to the Great Gun marsh site. Their cooperation during this study is gratefully acknowledged.

Funding for this study was provided by the National Park Service, NRPP-Natural Resource Management, under the guidance of Rebecca Beavers, coastal geomorphologist, NPS Geologic Resources Division.

# CHAPTER 1

## Evaluation of Marsh Development Processes at Fire Island National Seashore (New York): Purpose of the Study and Description of the Study Site

Contributing Authors: Charles T. Roman, John W. King, Donald R. Cahoon

---

### INTRODUCTION and PROBLEM STATEMENT

During the period of 1963 to 2003 the rate of global average sea level rise was  $1.8 \text{ mm yr}^{-1}$ , but it is predicted that with the influence of global climate change sea level could rise at a greatly accelerated rate, approaching a global average of  $4 \text{ mm y}^{-1}$  during the 2090-2099 period (Meehl et al. 2007). With sea level rise, marshes increase in vertical elevation and migrate, often landward (Redfield 1965). Under a regime of accelerated rates of sea level rise, the potential for submergence or loss of salt marsh habitat increases (e.g., Orson et al. 1985). In fact, there are extensive areas associated with the Mississippi delta region (Turner 1997) and portions of the Chesapeake Bay (Stevenson et al. 1985) where rates of sea level rise presently exceed vertical marsh accretion and marshes are being submerged. There is increasing evidence in the northeastern US indicating that some marsh sites may be at early stages of wetland submergence (Warren and Niering 1993, Roman et al. 1997, Donnelly and Bertness 2001). Salt marshes in New York City's Jamaica Bay are undergoing rapid conversion from vegetated wetland to mudflats (Hartig et al. 2002), with sea level rise identified as one of several contributing factors.

*Spartina*-dominated salt marshes (about 280-ha) fringe much of the Great South Bay back-barrier portions of Fire Island National Seashore (FIIS), a 50-km barrier island. There are no quantitative studies to document if these salt marshes are maintaining elevation relative to sea level rise; however, recent data assembled by the NY Department of Environmental Control suggests that back-barrier salt marshes to the west of Fire Island (Jamaica Bay) and elsewhere throughout the southern and Long Island Sound shores of Long Island are being lost by erosion and submergence processes (<http://www.dec.state.ny.us/website/dfwmr/marine/wetlands/index.html>). Salt marshes associated with Fire Island National Seashore provide essential nursery habitat for estuarine fishes (e.g., Bokuniewicz et al. 1993, Raposa and Oviatt 2000), shorebirds/waterbirds (Lent et al. 1990), and other trophic groups.

Given the ecological value of salt marshes and recent documentation that marshes nearby to FIIS and in the mid-Atlantic/northeast region are being lost, it is especially important to understand the processes that are controlling salt marsh maintenance within the Seashore and to obtain the ability to predict the future status of these estuarine habitats.

In addition to sea level rise, salt marsh development is especially sensitive to estuarine hydrology (frequency, duration, and depth of flooding) and sediment supply. In a back-barrier estuarine environment, like Great South Bay, these factors can dramatically change in response to geomorphic dynamics of the barrier island. For example, a recent hydrologic modeling exercise found that a storm-induced break in the Fire Island barrier would result in major changes to the hydrology and circulation of Great South Bay (Conley 2000). Predicted increases in mean tide elevations by as much as 2cm throughout the Bay will significantly alter the frequency, duration and depth of marsh surface flooding and delivery of sediment to the marsh surface, and thus, marsh development processes. Further, previous studies at Fire Island have clearly documented the role of inlets and overwash events (delivery of barrier island sediment to the back-barrier estuary) in establishing new areas for salt marsh establishment (Leatherman and Allen 1985).

The purpose of this study was to evaluate vertical marsh elevation change in relation to recent rates of sea level rise and to understand some of the factors or processes that are relevant to salt marsh development and maintenance.

The study relies on two principal methods.

- 1) Surface Elevation Tables and soil marker horizons (after Cahoon et al. 1995, 2002) were used to evaluate recent relationships between marsh surface elevation change and rates of relative sea-level rise. These methods also enable an understanding of surface and subsurface processes that contribute to marsh development (Chapter 2).
- 2) Radiometric dating of sediment cores, coupled with sedimentological analyses, enable an historic interpretation of marsh development processes (Chapter 3).

It is noted that in addition to vertical changes in marsh elevation with sea level rise, marshes can also migrate horizontally, encroaching seaward over tidal flats or landward over upland (Redfield 1965, Donnelly and Bertness 2001). This study was not designed to evaluate the horizontal dynamics associated with salt marsh development.

## **STUDY SITE**

The 50-km Fire Island is bounded by Fire Island Inlet to the west and Moriches Inlet to the east. It is hypothesized that salt marshes in the vicinity of these inlets are influenced by a different set of factors or magnitude of factors than marshes that are located away from inlets. Tidal range, tidal currents, and the potential for sediment transport are greater near inlets (Conley 2000) and these are all factors that are especially important in controlling marsh development. Also, marshes near portions of the barrier island with historic overwash episodes (e.g., Old Inlet portion of FIIS) may reflect different marsh development processes than those remote from overwash events. This produces a gradient of conditions that will be used in the project study design. Marsh development processes will be evaluated along a gradient from inlets to areas away from inlets.

Most of the present-day back-barrier salt marshes associated with Fire Island are on the eastern portion of the island, including the federal-designated Wilderness Area and the Smith Point County Park, a section of the barrier island where numerous inlets formed in the past providing substrate for marsh formation (Nordstrom and Jackson 2005, Psuty et al. 2005). Three marsh study areas (Fig. 1.1) were selected along a gradient from Moriches Inlet (Great Gun Meadows, 2.5 km from the Inlet; Hospital Point, 12 km; Watch Hill 20 km). The sites established remote from Moriches Inlet, Watch Hill and Hospital Point, were also remote from Fire Island Inlet, 29 km and 37 km, respectively.

No tide elevation data are available for the specific marsh study sites, but based on existing tide records from throughout Moriches Bay, Great South Bay and the inlets (Fig. 1.2), tidal range at the three marsh sites can be inferred. Great Gun, located in Moriches Bay and near the inlet probably has a mean tidal range that is <66cm (Moriches Coast Guard) and >37cm (Smith Pt. Bridge). The Hospital Point and Watch Hill marsh sites probably have a mean tidal range that reflects the tide station sites in Great South Bay (18 – 21 cm), with Hospital Point perhaps greater than Watch Hill due to its closer proximity to Moriches Inlet.

Based on historic records and an analysis of physiographic features, Leatherman and Allen (1985) have described the recent history (past 200 years) of inlets throughout Fire Island. With the delivery of sediment from the ocean to the bay and creation of flood-tidal deltas, inlets are particularly important to the formation of barrier island salt marshes (e.g., Fisher and Simpson 1979, Leatherman 1979, Leatherman and Allen 1985, Roman and Nordstrom 1988). Historically, there were persistent inlets located in the immediate vicinity of the three study marshes (Fig. 1.3).

Overwash processes are also important to the bayward transport of sediment and ultimate marsh development; however, Leatherman and Allen (1985) report that historically on Fire Island overwash events rarely crossed the entire island and deposited sediment to the bay forming a platform for marsh colonization. Flood tidal deltas, associated with inlets, appear to be an important geomorphic event contributing to marsh development at Fire Island. It is noted that the September 1938 hurricane crossed the island at Moriches Inlet, resulting in five short-lived inlets within 2.4 km to the east of the Inlet and extensive overwash west of the Inlet (i.e., near the marsh study sites; Leatherman and Allen 1985). Also, during two nor'easters (October 1991 and December 1992) there were overwash events at Old Inlet.

## **LITERATURE CITED**

Bokuniewicz, H., A. McElroy, C. Schlenk, and J. Tanski, eds. 1993. Estuarine resources of the Fire Island National Seashore and vicinity. Final report to the National Park Service. NY Sea Grant Institute, Stony Brook, NY.

Cahoon, D.R., D.J. Reed, and J.W. Day, Jr. 1995. Estimating shallow subsidence in microtidal salt marshes of the southeastern United States: Kaye and Barghoorn revisited. *Marine Geology* 128: 1-9.

Cahoon, D.R., J.C. Lynch, B.C. Perez, B. Segura, R. Holland, C. Stelly, G. Stephenson, and P. Hensel. 2002. A device for high precision measurement of wetland sediment elevation: II. The rod surface elevation table. *Journal of Sedimentary Research* 72: 734-739.

Conley, D.C. 2000. Numerical modeling of Fire Island storm breach impacts upon circulation and water quality of Great South Bay, NY. Technical Report NPS/BSO-RNR/NRTR/00-10. National Park Service, New England System Support Office, Boston, MA.

Donnelly, J.P., and M.D. Bertness. 2001. Rapid shoreward encroachment of salt marsh cordgrass in response to accelerated sea-level rise. *Proceedings of the National Academy of Sciences* 98: 14218-14223.

Fisher, J.J., and E. J. Simpson. 1979. Washover and tidal sedimentation rates as environmental factors in development of a transgressive barrier shoreline. Pages 127 – 148 in *Barrier Islands from the Gulf of St. Lawrence to the Gulf of Mexico* (S.P. Leatherman, ed.). Academic Press, NY.

Hartig, E.K., V. Gronitz, A. Kolker, F. Muchacke, and D. Fallon. 2002. Anthropogenic and climate-change impacts on salt marshes of Jamaica Bay, New York City. *Wetlands* 22: 71-89.

Leatherman, S.P. 1979. Migration of Assateague Island, Maryland, by inlet and overwash processes. *Geology* 7: 104-107.

Leatherman, S.P., and J.R. Allen, eds. 1985. *Geomorphic analysis: Fire Island Inlet to Montauk Point, Long Island, New York*. NPS Technical Report to the US Army Corps of Engineers, NY District.

Lent, R.A., T. Hruby, and D.F. Cowan. 1990. *Open Marsh Water Management on Great South Bay, Islip, New York*. Final Report. Seatuck Foundation, Cornell University, Islip, NY.

Meehl, G.A., T.F. Stocker, W.D. Collins, P. Friedlingstein, A.T. Gaye, .M. Gregory, A. Kitoh, R. Knutti, J.M. Murphy, A. Noda, S.C.B. Raper, I.G. Watterson, A.J. Weaver, and Z.C. Zhao. 2007. Global Climate Projections, Chapter 10. Pages 747-822 in *Climate Change 2007: The Physical Science Basis. Contribution of Working Group I to the Fourth Assessment Report of the Intergovernmental Panel on Climate Change* (Solomon, S., D. Qin, M. Manning, Z. Chen, M. Marquis, K.I.B. Averyt, M. Tignor and H.L. Miller, editors). Cambridge University Press, Cambridge, United Kingdom and New York, NY.

Nordstrom, K.F., and N.L. Jackson. 2005. Bay shoreline physical processes (Fire Island National Seashore science synthesis paper. Technical Report NPS/NER/NRTR-2005/020. National Park Service, Boston, MA.

Orson, R., W. Panageotou, and S.P. Leatherman. 1985. Response of tidal salt marshes of the U.S. Atlantic and Gulf coasts to rising sea levels. *Journal of Coastal Research* 1: 29-37.

Psuty, N.P., M. Grace, and J.P. Pace. 2005. The coastal geomorphology of Fire Island: a portrait of continuity and change (Fire Island National Seashore science synthesis paper. Technical Report NPS/NER/NRTR-2005/021. National Park Service, Boston, MA.

Raposa, K.B., and C.A. Oviatt. 2000. The influence of contiguous shoreline type, distance from shore, and vegetation biomass on nekton community structure in eelgrass beds. *Estuaries* 23: 46-55.

Redfield, A.C. 1965. Ontogeny of a salt marsh estuary. *Science* 147: 50-55.

Roman, C.T., and K.F. Nordstrom. 1988. The effect of erosion rate on vegetation patterns of an East Coast barrier island. *Estuarine, Coastal and Shelf Science* 26: 233-242.

Roman, C.T., J.A. Peck, J.R. Allen, J.W. King, and P.G. Appleby. 1997. Accretion of a New England (USA) salt marsh in response to inlet migration, storms, and sea-level rise. *Estuarine, Coastal and Shelf Science* 45: 717-727.

Stevenson, J.C., M.S. Kearney, and E.C. Pendleton. 1985. Sedimentation and erosion in a Chesapeake Bay brackish marsh system. *Marine Geology* 67: 213-235.

Turner, R.E. 1997. Wetland loss in the northern Gulf of Mexico: multiple working hypotheses. *Estuaries* 20: 1-13.

Warren, R.S., and W.A. Niering. 1993. Vegetation change on a northeast tidal marsh: interaction of sea-level rise and marsh accretion. *Ecology* 74: 96-103.

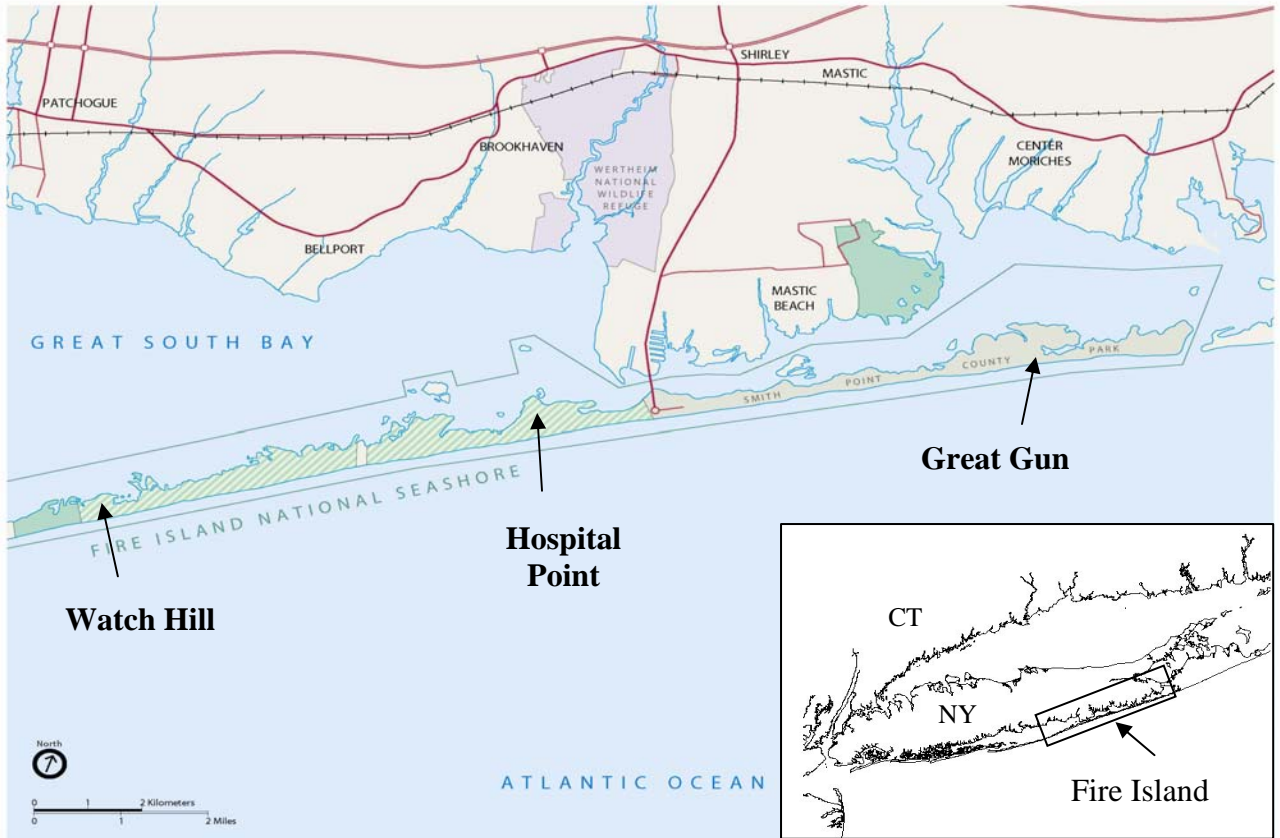


Fig. 1.1. Regional location of the three marsh study sites at the eastern end of Fire Island.



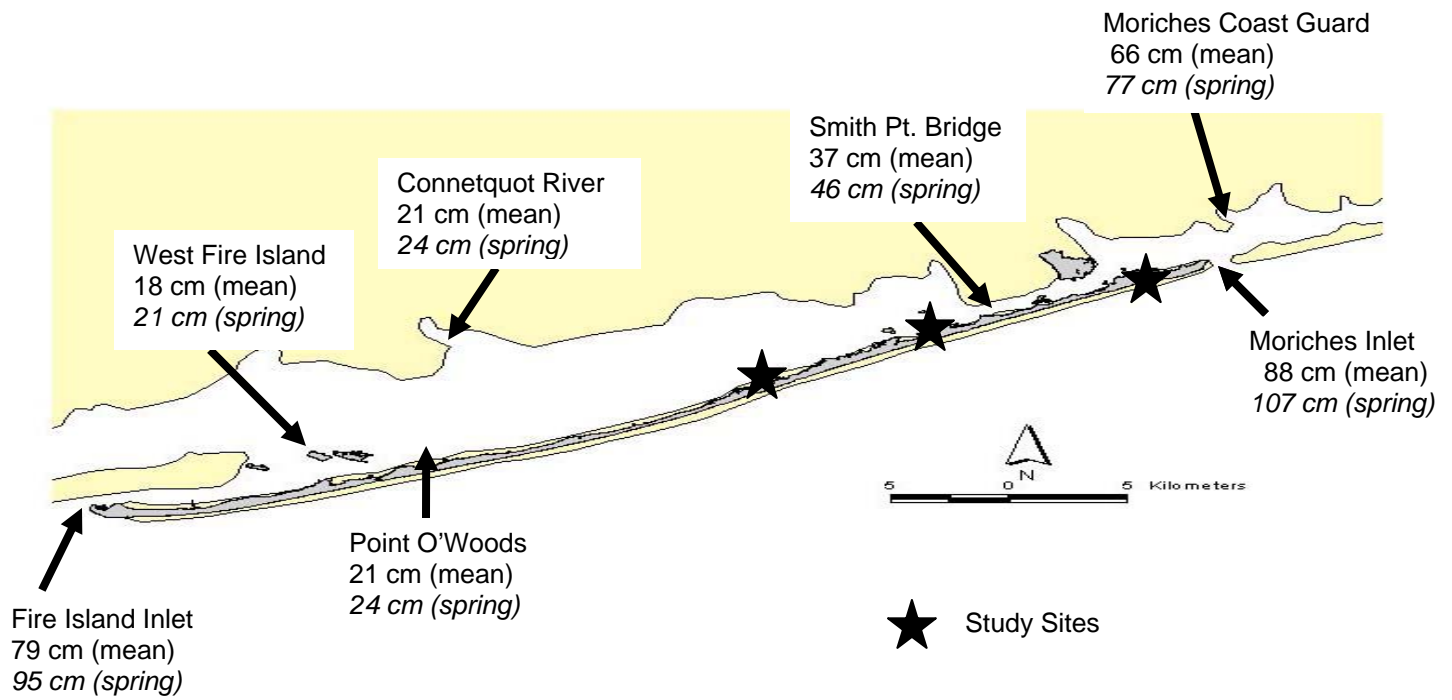


Fig. 1.2. Mean and spring tide range at various locations throughout Great South Bay and the inlets. Data source: NOAA-NOS, tidal station locations and ranges, <http://140.90.121.756/tides05/tab2ec2a.html>

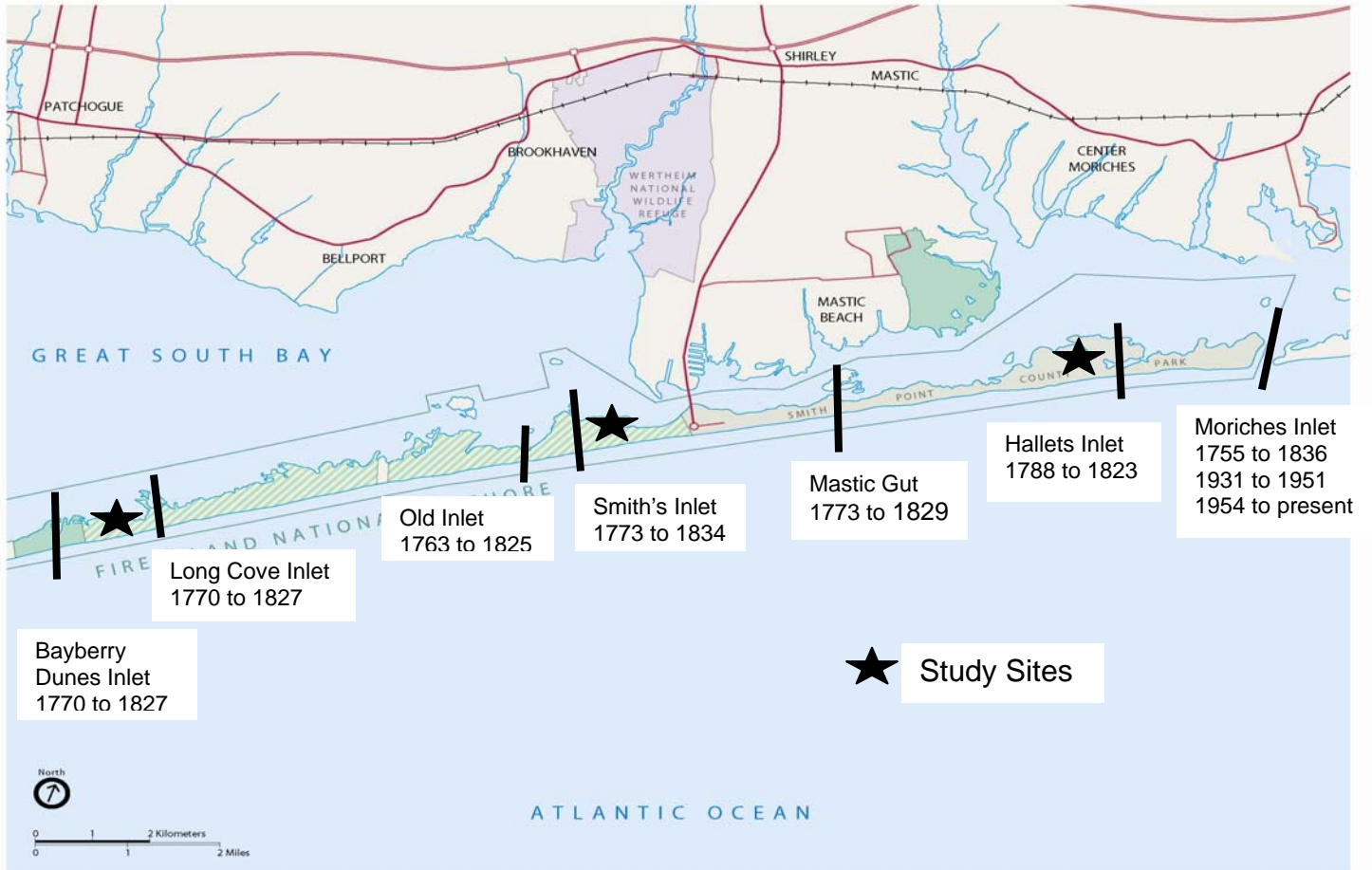


Fig. 1.3. Location of historic inlets within the vicinity of the three marsh study sites. Source: Leatherman and Allen 1985.

## CHAPTER 2

### Monitoring Marsh Surface Elevation Change and Evaluating the Role of Surface and Subsurface Processes

Contributing Authors: Charles T. Roman, Donald R. Cahoon and James C. Lynch

---

#### INTRODUCTION to the SET and MARKER HORIZON METHOD

The elevation of a salt marsh is controlled by sediment accretion and organic matter build-up, which result in increases in elevation, while the subsurface processes of sediment compaction/subsidence and organic matter decomposition, as well as erosion of surface sediments can result in elevation loss. Boumans and Day (1993) and Cahoon et al. (1995a, 1999) present a method whereby surface accretionary processes are monitored by repeated sampling of artificial marker horizon plots and marsh surface elevation is correspondingly monitored with a surface elevation table (SET) (Cahoon et al. 2002a). This method enables an interpretation of how surface processes (deposition and erosion) and subsurface processes (compaction, decomposition, organic matter accumulation) influence marsh elevation.

Each individual SET station contains a benchmark rod that is driven through the marsh peat and into the underlying sediment, often 10m or deeper, providing a constant reference elevation (Fig. 2.1). The SET is then attached to the benchmark pipe and pins are lowered to the marsh surface. Repeated pin measurements, always in the same location, record changes in marsh surface elevation. All measurements are relative to the benchmark elevation, which remains constant through time. After taking measurements, the SET is removed from the benchmark. Simultaneous with the SET measurements, marker horizons are used to measure surface deposition or surface erosion of material. Conceptually, if from time  $a$  to time  $b$ , an increase in marsh surface elevation was recorded from the SET readings, and the same increase was noted from accumulation of material above the marker horizon, it could be suggested that the marsh surface elevation increase was primarily due to the surface process of sediment deposition. If from time  $a$  to time  $b$  there was an increase in marsh surface elevation from the SET readings that was greater than the vertical accretion above the marker horizon, then the subsurface processes of belowground growth of roots and rhizomes and/or porewater storage could be contributing to the marsh surface elevation increase. Finally, if the vertical accretion was greater than the marsh surface elevation change measured from the SET, then

subsurface processes of organic matter decomposition, compaction, and perhaps porewater flux may be factors contributing to the shallow subsidence.

## METHODS

### Field and Laboratory Methods

At each of the three marsh study areas, three sites for individual SET stations were located in a random manner (Fig. 2.2, Table 2.1). All individual SET sites were located in *Spartina alterniflora* and/or *Spartina patens* vegetation and at least 5 m from tidal creeks, ditches or the bay fronts.

Benchmarks for the rod-type SETs (Cahoon et al. 2002b) were installed July 23-24, 2002. Depth of the benchmarks ranged from 14.6m to 17.1m below the marsh surface (Table 2.1). Initial SET marsh surface elevation readings were made August 14, 2002 and commenced thereafter at 3-4 month intervals during the spring through fall period, except in 2006 when only one measurement was made in September.

|      |            |
|------|------------|
| 2002 | Aug 14-15  |
|      | Nov 13-14  |
| 2003 | Apr 2-3    |
|      | Jul 14-15  |
|      | Oct 24     |
| 2004 | Apr 29-30  |
|      | Jul 19-20  |
|      | Nov 3-4    |
| 2005 | Jun 15-16  |
|      | Oct 20     |
| 2006 | Sept 18-19 |
| 2007 | May 15-16  |

Methods of SET benchmark installation and routine sampling followed Cahoon et al. (2002a & b). In brief, at each sampling event the SET is firmly attached to the top of the benchmark pipe. The horizontal arm of the SET contains 9 fiberglass pins that are lowered to the marsh surface to measure elevation relative to the benchmark pipe with an accuracy of  $\pm 1.5$ mm. Pin readings are taken at four fixed positions for each benchmark. After reading, the SET is removed from the benchmark. At each SET site, 3 circular feldspar marker horizon plots (45cm diameter) were established August 14-15, 2002. Subsequent sampling of the marker horizon was by the cryogenic coring technique after Cahoon et al. (1996) and occurred simultaneous with the SET readings. Portable boardwalks were used at each site to avoid trampling of the marsh surface.

In addition to the cited publications, the following website contains information on the concepts and theory of the SET and marker horizon methods and details on installation and measurements (<http://www.pwrc.usgs.gov/set/>).

During the September 18-19, 2006, sampling date the material that was accumulated above the feldspar marker horizon was collected to determine organic/inorganic composition. After obtaining the cryo-core at each feldspar plot, the material above the feldspar horizon was collected (see Fig. 2.1 for a view of material accumulated above the feldspar horizon). In the laboratory, material collected from each replicate feldspar plot, at each SET site, was pooled for analysis (e.g., Hospital Point SET#1, feldspar plots 1, 2, and 3 were pooled). Organic content was determined by loss-on-ignition after Dean (1974). Data are presented as mean and standard error for each marsh study area (e.g., mean of Hospital Point SET#1, SET#2, and SET#3).

## **Data Analysis**

For each site and for each of the 12 sample dates, each SET was a replicate, thus  $n=3$ . For measuring vertical accretion with the marker horizon method, the sample size was similarly 3. Marsh surface elevation change rates and rates of vertical accretion were derived from linear regression (e.g., regression coefficient). Rates of elevation change and vertical accretion rates were compared among sites by Analysis of Variance (ANOVA), followed by a post-hoc multiple contrast test. Differences in elevation change and vertical accretion rates for each site were determined by ANOVA.

## **RESULTS and DISCUSSION**

### **Marsh Elevation, Vertical Accretion, and Shallow Subsidence**

After nearly 5 years of monitoring, vertical accretion (measured by the feldspar marker horizons) was greater than the marsh surface elevation at all sites (Fig. 2.3; Great Gun accretion vs elevation,  $p=0.0023$ ; Hospital Point  $p<0.0001$ ; Watch Hill  $p<0.0001$ ). Although sediment accumulated on the marsh surface (vertical accretion), the elevation of the marsh surface did not reflect this accumulation. At the Watch Hill site, and to some degree at Hospital Point, accumulation of sediment on the marsh surface and the increase in elevation were similar until the last several sampling events. However, divergence between surface accretion and marsh elevation was strong at the Great Gun marsh site. This difference is termed shallow subsidence (accretion minus elevation). Belowground processes occurring between the marsh surface and the bottom of the benchmark (14-17m deep) are contributing to shallow subsidence. Factors such as autocompaction of marsh sediments, decomposition of belowground organic matter, and changes in belowground water storage may likely be contributing to the elevation deficit. This study was not designed to differentiate among these and other belowground processes.

Shallow subsidence (when surface accretion is greater than elevation gain) is reported as a fairly common occurrence in coastal wetlands. In a review of findings from 43 sites located throughout coastal North America and Western Europe, about 45% of the sites

revealed significant shallow subsidence, while almost 50% of the sites showed that elevation and accretion were equivalent (Cahoon et al. 1999).

### **Relation of marsh surface elevation to sea level rise**

Salt marshes are intertidal habitats, tightly coupled to mean sea level (Redfield 1965). Salt marsh vegetation patterns in the southern New England/Long Island area range from the low marsh elevations with daily tidal flooding to less frequently flooded high marsh (Taylor 1938, Niering and Warren 1980). *Spartina alterniflora* occurs in this low marsh zone, along margins of tidal creeks, ditches, and often the bay-front. The more extensive meadows of the high marsh are generally flooded by astronomical spring tides and storm tides, with vegetation dominated by short-form *Spartina alterniflora*, *Spartina patens*, and others. *Spartina alterniflora* can tolerate frequent flooding of the low marsh environment because of a network of intercellular spaces that serve to deliver oxygen from above-ground plant parts to below-ground roots (Teal and Kanwisher 1966). High marsh plants, like *Spartina patens* and *Distichlis spicata*, lack this ability and are restricted to the better drained high marsh environments.

For marshes to be maintained under a regime of rising sea level, marsh surface elevation must keep pace. If sea level rise is greater than marsh elevation increases, the marsh could become submerged. With submergence the soils become waterlogged and anaerobic soil conditions persist. Under anaerobic conditions high concentrations of hydrogen sulfide can become toxic to root metabolism, inhibiting nitrogen uptake and resulting in decreased plant growth (Howes et al. 1986, Koch et al. 1990). With aerenchyma tissue *Spartina alterniflora* is adapted to these flooded conditions and under severely reducing conditions this species can respire anaerobically (Mendelssohn et al. 1981). However, under a regime of prolonged flooding and anoxic soil conditions stress on the plants will become severe leading to plant death, collapse of peat, and ultimate increased flooding (DeLaune et al. 1994).

During the study period, from August 2002 to May 2007, elevation change of the marsh surface ranged from an increase of 2.04 mm y<sup>-1</sup> and 2.08 mm y<sup>-1</sup> at Hospital Point and Watch Hill, respectively, to an elevation decline of -1.05 mm y<sup>-1</sup> at Great Gun (Table 2.2, Fig. 2.3). There are no long-term records of sea level within the Great South Bay or Moriches Bay study area, but long-term records of relative sea level from NOAA water level stations in the vicinity range from 2.52 mm y<sup>-1</sup> to 3.79 mm y<sup>-1</sup> (Table 2.3, Fig. 2.4). The long-term relative sea level rise rate at Sandy Hook, NJ, (about 95 km west of Watch Hill) is greater than rates at The Battery (southern end of Manhattan Island; 95 km from Watch Hill) or Montauk Point (eastern end of Long Island, 90 km from Watch Hill). Psuty et al. (2005) argues that the Sandy Hook water level record is most applicable to Fire Island because of similar barrier island settings. Wong and Wilson (1984) suggest sea-level fluctuations along the entire coast from Sandy Hook to Montauk Point are similar in phase. But regardless of the long-term relative rate that is applied for comparison with the Fire Island marsh surface elevation data, all three sites are revealing an elevation deficit. If only vertical accretion were measured at the study sites, it could

be suggested that the marshes are nearly keeping pace with relative sea level rise (accretion rates ranged from 2.12 to 3.76 mm y<sup>-1</sup>; Table 2.2), but this would be an erroneous conclusion because of the substantial shallow subsurface subsidence at the sites. Cahoon et al. (1995a) advise that both marsh surface elevation and vertical accretion data be collected simultaneously as done in this Fire Island study.

Calculated marsh surface elevation deficits in relation to the rate of relative sea-level rise should be interpreted with caution. The marsh elevation and accretion data set reported in this paper is 58 months duration, a relatively short time period that is not adequate to integrate the complexity of processes, of both short-term or episodic and long-term duration that control marsh surface elevation. For example, there is a history of numerous inlets in the vicinity of the three marsh study areas (Fig. 1.3), a principal mechanism of sediment delivery to the bays, but during the study period there were no major hurricanes or nor'easters. There are reports of substantial deposits of sediment on the marsh surface in association with storms (e.g., Stumpf 1983, Cahoon et al. 1995b, Roman et al. 1997, Donnelly et al. 2004).

The temporal pattern of mean sea-level is quite variable (see Fig. 2.4), but it is thought that long-term marsh processes, such as belowground primary production and daily surface accretion/erosion processes, are not able to adjust quickly to these interannual fluctuations, thus marshes may be in a state of constant disequilibrium in relation to mean sea-level (Bricker-Urso et al. 1989, Morris et al. 2002). The rate of relative sea-level rise at the Sandy Hook water level station during the 58 month study duration, was -10.85 mm y<sup>-1</sup> (regression of annual average sea-level; R<sup>2</sup> 0.14, *p* = 0.46 NS), perhaps representing a time-period when the marsh is able to respond or adjust to previous periods of rapid sea-level rise (e.g., the rate of rise for the 10-yr period, 1992-2001, prior to the study was 3.56 mm y<sup>-1</sup>, R<sup>2</sup> 0.16, *p* = 0.25 NS). At a USGS-operated water level station at the western end of Great South Bay (Lindenhurst, NY) that has been in operation only since 2002, the rate during the 58-month study duration was, as expected, similar to Sandy Hook at -9.84 mm y<sup>-1</sup> (Table 2.3). The time-frame for salt marsh development processes to adjust to changes in the rate of sea-level rise is not known, but it is clear that given the year-to-year variability in sea-level rise it is important to evaluate marsh elevation dynamics over the long-term, enabling a record of the marsh response to episodes of both high rates of sea-level rise and slower rates of rise. It is noted that the short-term rates of sea-level rise presented here (10-yr rate at Sandy Hook and 58-month rates) are quite variable, none of the trends are statistically significant, and thus, they should be interpreted with caution. This is why we initially compared the marsh elevation and accretion trends over the 58-month study period with the longer-term records of sea-level from the region's water level stations.

The Fire Island marsh study sites are in an elevation deficit, relative to the long-term rate of sea-level rise at Sandy Hook. This deficit trend could continue for the long-term, there could be a pulse of sediment delivered to the marsh surface during a future storm event, or as noted above, the marshes may have the capacity to periodically adjust, over the long-term, during episodes of low rates of sea-level rise. Over the next century the rate of sea-level rise is predicted to accelerate in response to global warming (Gornitz 1995,

Meehl et al. 2007) and continued monitoring of marsh elevation and accretion, relative to sea-level, will be necessary to evaluate the long-term consequences of this predicted rise on marsh development processes.

### **Relation of marsh surface elevation to sea level rise: Special comments for the Great Gun marsh site**

Given that the Great Gun marsh site shows a substantial elevation deficit in relation to relative sea-level rise, some special mention is warranted. Three replicate SET benchmark stations were established at each marsh study site and at Great Gun there was considerable variability among the replicates (Fig. 2.5). SET benchmarks #1 and #2 showed a trend of decreased elevation over the 58 month study period, while SET #3 showed elevation gain that was similar in magnitude to all of the replicate SETs at Hospital Point and Watch Hill, except for Hospital Point SET#1 (General Linear Model with multiple contrast tests  $p \leq 0.05$ ). When the three benchmark sites were established, the field team located a large portion of marsh that was fairly uniform and then randomly selected sites for the three SET replicates. At the start of the study in August 2002 the three SET benchmark sites at Great Gun appeared similar, although SET #3 was within *Spartina patens*/short *Spartina alterniflora* vegetation and SETs #1 and #2 were *Spartina alterniflora* of intermediate stature (perhaps 1m), suggesting a subtle elevation gradient. We expect that the observed elevation deficit trend at SETs #1 and #2 is localized and not common throughout the Great Gun marsh complex. Over the five year duration of the study we have observed that the SET #1 and #2 marsh locations appear to be getting wetter, perhaps due to initiation of a natural marsh drainage channel.

### **Marsh elevation change and vertical accretion vary among the study sites**

This study was designed to determine if marsh development processes vary at Fire Island along a gradient from sites near inlets to those remote from inlets. Mean tidal range is greater at Great Gun (between 37 and 66 cm) than at Hospital Point or Watch Hill (18-21 cm), sites remote from Moriches Inlet (Fig. 1.2). In a review of 16 marshes located along the Atlantic and Gulf of Mexico coasts from Massachusetts to Louisiana there is a reported positive relationship between tidal range and accretion (Stevenson et al. 1986); however, studying salt marshes along the Atlantic coast of Canada the opposite trend was noted (Chmura and Hung 2004). At Fire Island, the Great Gun site had a significantly lower rate of vertical accretion and a significant decline in elevation when compared to the Hospital Point and Watch Hill sites (Table 2.2), but we offer no evidence to suggest that this trend is related to mean tidal range.

It was noted that the material that accumulated above the feldspar marker horizon during the period of August 2002 to September 2006 was 52% (2.7% SE) and 56% organic content (0.6% SE) at Hospital Point and Watch Hill respectively, while at Great Gun, nearer the influence of Moriches Inlet, the organic content was lower (29%, 6.9% SE). Organic material accumulation is important to the marsh development process as



determined elsewhere (e.g., Bricker-Urso et al. 1989, Nyman et al. 2006). Sparse *Spartina alterniflora* vegetation cover, and thus lower biomass of roots/rhizomes at the Great Gun site (not quantified) may be a factor in the lower organic content of accumulated material, and ultimately contributing to the elevation deficit at Great Gun SET sites #1 and #2.

### **Long-Term Monitoring of Marsh Development Processes**

Salt marshes are dynamic environments, with the habitat structure and vegetation patterns changing in response to sea level rise and sediment transport processes (e.g., Donnelly and Bertness 2001), altered hydrology (e.g., Roman et al. 1984, Adamowicz and Roman 2005), climate change (e.g., air temperature; Bertness 1999), nutrient loading (e.g., Nixon and Oviatt 1973), and other factors. The National Park Service Northeast Coastal and Barrier Network proposes a comprehensive monitoring program for salt marsh and estuarine habitats, including marsh development process monitoring with SETs and feldspar marker horizons, along with vegetation and marsh landscape change monitoring, nutrient loading and eutrophication monitoring, and resident fish monitoring. With this multiple parameter approach, as vegetation patterns change or habitat structure is altered (e.g., increased open water habitat on the marsh surface), managers will have at least an initial understanding of why the ecosystem is changing, perhaps in response to an elevation deficit, nutrient loading, altered hydrology, or other factors. This knowledge of possible causes of marsh landscape change could enable the development of more informed or targeted research questions and ultimate management action, if warranted. Given that the global rate of sea-level rise is expected to accelerate over the next century (Gornitz 1995, Meehl et al 2007), and that some marshes in the northeast are becoming submerged (Hartig et al. 2002) or show evidence of submergence (e.g., Stevenson et al. 1985, Warren and Niering 1993, Donnelly and Bertness 2001), it is especially important to continue monitoring of marsh elevation changes in response to sea-level rise.

### **LITERATURE CITED**

Adamowicz, S.C., and C.T. Roman. 2005. New England salt marsh pools: a quantitative analysis of geomorphic and geographic features. *Wetlands* 25: 279-288.

Bertness, M.D. 1999. *The Ecology of Atlantic Shorelines*. Sinauer Associates, Inc., Sunderland, MA.

Boumans, R., and J.W. Day, Jr. 1993. High precision measurements of sediment elevation in shallow coastal areas using a sedimentation-erosion table. *Estuaries* 16: 375-380.

Bricker-Urso, S., S.W. Nixon, J.K. Cochran, D.J. Hirschberg, and C. Hunt. 1989. Accretion rates and sediment accumulation in Rhode Island salt marshes. *Estuaries* 12: 300-317.

Cahoon, D.R., J.W. Day, Jr., and D.J. Reed. 1999. The influence of surface and shallow subsurface soil processes on wetland elevation: a synthesis. *Current Topics in Wetland Biogeochemistry* 3: 72-88.

Cahoon, D.R., D.J. Reed, and J.W. Day, Jr. 1995a. Estimating shallow subsidence in microtidal salt marshes of the southeastern United States: Kaye and Barghoorn revisited. *Marine Geology* 128: 1-9.

Cahoon, D.R., D.J. Reed, J.W. Day, Jr., G.D. Steyer, R. Boumans, J.C. Lynch, D. McNally, and N. Latif. 1995b. The influence of Hurricane Andrew on sediment distribution in Louisiana coastal marshes. *Journal of Coastal Research* 21: 280-294.

Cahoon, D.R., J.C. Lynch, and R.M. Knaus. 1996. Improved cryogenic coring device for sampling wetland soils. *Journal of Sedimentary Research* 66: 1026-1027.

Cahoon, D. R., J. C. Lynch, P. Hensel, R. Boumans, B. C. Perez, B. Segura, J. W. Day, Jr., 2002a. High precision measurement of wetland sediment elevation: I. recent improvements to the Sedimentation-Erosion Table. *Journal of Sedimentary Research* 72: 730-733.

Cahoon, D.R., J.C. Lynch, B.C. Perez, B. Segura, R. Holland, C. Stelly, G. Stephenson, and P. Hensel. 2002b. A device for high precision measurement of wetland sediment elevation: II. The rod surface elevation table. *Journal of Sedimentary Research* 72: 734-739.

Chmura, G.L., and G.A. Hung. 2004. Controls on salt marsh accretion: a test in salt marshes of Eastern Canada. *Estuaries* 27: 70-81.

Dean, W. E. 1974. Determination of carbonate and organic matter in calcareous sediments and sedimentary rocks by loss on ignition: comparison with other methods. *Journal of Sedimentary Petrology* 44: 242-248.

DeLaune, R.D., J.A. Nyman, and W.H. Patrick, Jr. 1994. Peat collapse, ponding and wetland loss in a rapidly submerging coastal marsh. *Journal of Coastal Research* 10: 1021-1030.

Donnelly, J.P., and M.D. Bertness. 2001. Rapid shoreward encroachment of salt marsh cordgrass in response to accelerated sea-level rise. *Proceedings of the National Academy of Sciences* 98: 14218-14223.

Donnelly, J.P., J. Butler, S. Roll, M. Wengren, and T. Webb III. 2004. A backbarrier overwash record of intense storms from Brigantine, New Jersey. *Marine Geology* 107-121.

Gornitz, V. 1995. Sea-level rise: a review of recent, past and near-future trends. *Earth Surface Processes and Landforms* 20: 7-20.

Hartig, E.K., V. Gronitz, A. Kolker, F. Muchacke, and D. Fallon. 2002. Anthropogenic and climate-change impacts on salt marshes of Jamaica Bay, New York City. *Wetlands* 22: 71-89.

Howes, B.L., J.W.H. Dacey, and D.D. Goehring. 1986. Factors controlling the growth form of *Spartina alterniflora*: feedbacks between above-ground production, sediment oxidation, nitrogen, and salinity. *Journal of Ecology* 74: 881-898.

Koch, M.S., I.A. Mendelssohn, and K.L. McKee. 1990. Mechanism for the hydrogen-sulfide-induced growth limitation in wetland macrophytes. *Limnology and Oceanography* 35: 399-408.

Meehl, G.A., T.F. Stocker, W.D. Collins, P. Friedlingstein, A.T. Gaye, .M. Gregory, A. Kitoh, R. Knutti, J.M. Murphy, A. Noda, S.C.B. Raper, I.G. Watterson, A.J. Weaver, and Z.C. Zhao. 2007. Global Climate Projections, Chapter 10. Pages 747-822 in *Climate Change 2007: The Physical Science Basis. Contribution of Working Group I to the Fourth Assessment Report of the Intergovernmental Panel on Climate Change* (Solomon, S., D. Qin, M. Manning, Z. Chen, M. Marquis, K.I.B. Averyt, M. Tignor and H.L. Miller, editors). Cambridge University Press, Cambridge, United Kingdom and New York, NY.

Mendelssohn, I.A., K.L. McKee, and W.H. Patrick, Jr. 1981. Oxygen deficiency in *Spartina alterniflora* roots: metabolic adaptation to anoxia. *Science* 214: 439-441.

Morris, J.T., P.V. Sundareshwar, C.T. Nietch, B. Kjerfe, and D.R. Cahoon. 2002. Responses of coastal wetlands to rising sea level. *Ecology* 83: 2869-2877.

Niering, W.A., and R.S. Warren. 1980. Vegetation patterns and processes in New England salt marshes. *BioScience* 30: 301-307.

Nixon, S.W., and C.A. Oviatt. 1973. Analysis of local variation in the standing crop of *Spartina alterniflora*. *Botanica Marina* 16: 103-109.

Nyman, J.A., R.J. Walters, R.D. Delaune, and W.H. Patrick, Jr. 2006. Marsh vertical accretion via vegetative growth. *Estuarine Coastal and Shelf Science* 69: 370-380.

Psuty, N.P., M. Grace, and J.P. Pace. 2005. The coastal geomorphology of Fire Island: a portrait of continuity and change. Technical Report NPS/NER/NRTR-2005/021. National Park Service, Boston, MA.

- Redfield, A.C. 1965. Ontogeny of a salt marsh estuary. *Science* 147: 50-55.
- Roman, C.T., W. A. Niering, and R. S. Warren. 1984. Salt marsh vegetation change in response to tidal restriction. *Environmental Management* 8: 141-150.
- Roman, C.T., J.A. Peck, J.R. Allen, J.W. King, and P.G. Appleby. 1997. Accretion of a New England (USA) salt marsh in response to inlet migration, storms, and sea-level rise. *Estuarine, Coastal and Shelf Science* 45: 717-727.
- Stevenson, J.C., M.S. Kearney, and E.C. Pendleton. 1985. Sedimentation and erosion in a Chesapeake Bay brackish marsh system. *Marine Geology* 67: 213-235.
- Stevenson, J.C., L.G. Ward, and M.S. Kearney. 1986. Vertical accretion in marshes with varying rates of sea level rise, pages 241-259. In *Estuarine Variability* (D.A. Wolfe, ed.). Academic Press, Inc., Orlando.
- Stumpf, R.P. 1983. The process of sedimentation on the surface of a salt marsh. *Estuarine, Coastal and Shelf Science* 17: 495-508.
- Taylor, N. 1938. A preliminary report on the salt marsh vegetation of Long Island, New York, pages 21-84. In *New York State Museum Bulletin*, No. 316, Albany, NY.
- Teal, J.M., and J.W. Kanwisher. 1966. Gas transport in the marsh grass, *Spartina alterniflora*. *Journal of Experimental Botany* 17: 355-361.
- Warren, R.S., and W.A. Niering. 1993. Vegetation change on a northeast tidal marsh: interaction of sea-level rise and marsh accretion. *Ecology* 74: 96-103.
- Wong, K.C., and R.E. Wilson. 1984. Observations of low-frequency variability in Great South Bay and relations to atmospheric forcing. *Journal of Physical Oceanography* 14: 1893-1900.

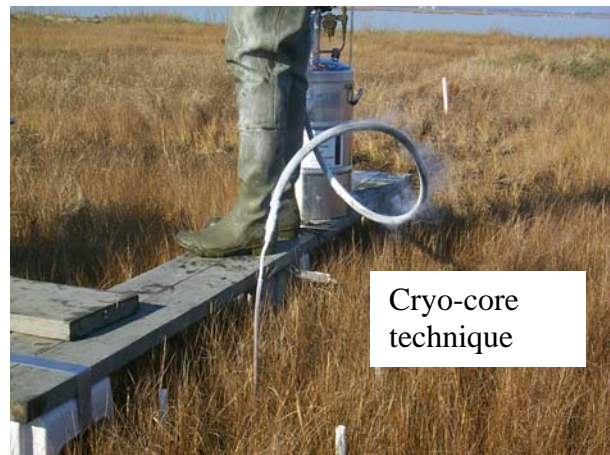
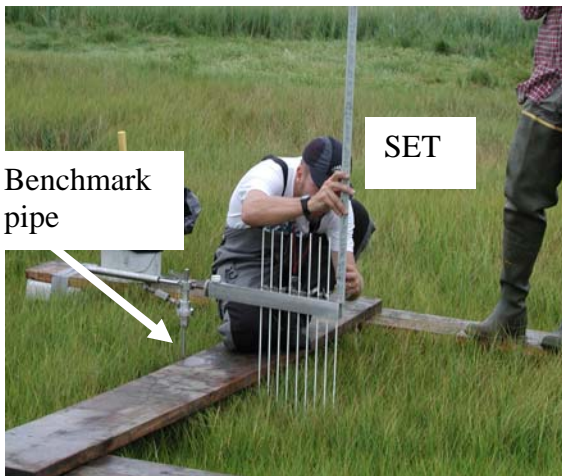
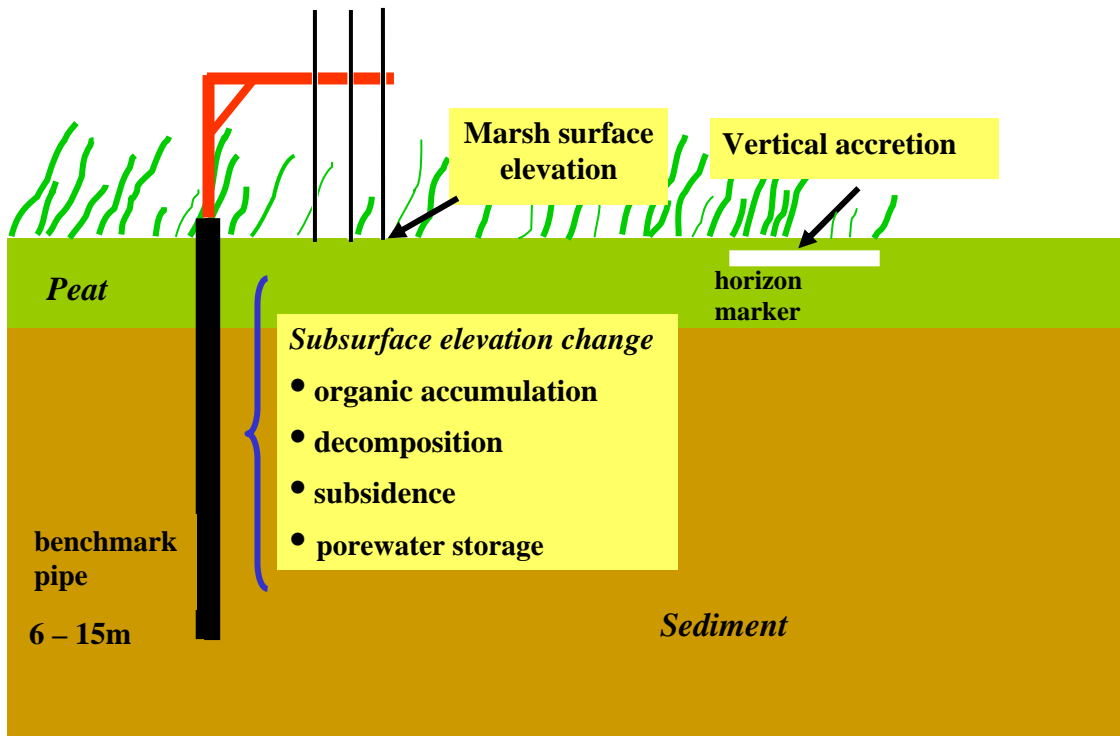


Fig. 2.1.

Top – Schematic of the SET and horizon marker sample design.

Photographs of rod-type SET with nine measuring pins, sampling of marsh surface horizon using the cryogenic-core technique, and a cryo-core sample showing feldspar marker horizon and sediment that has accumulated above the horizon.



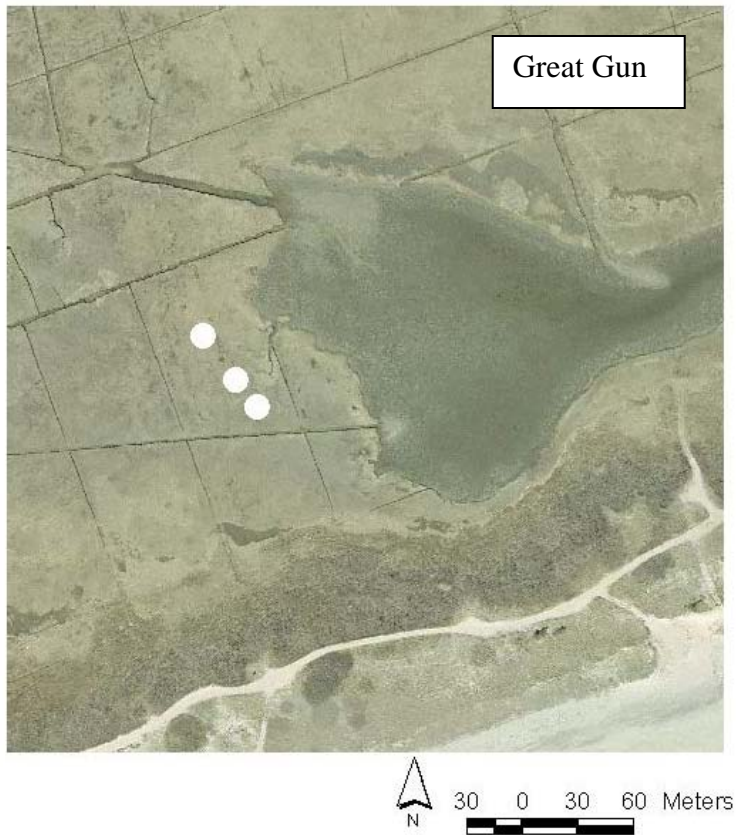
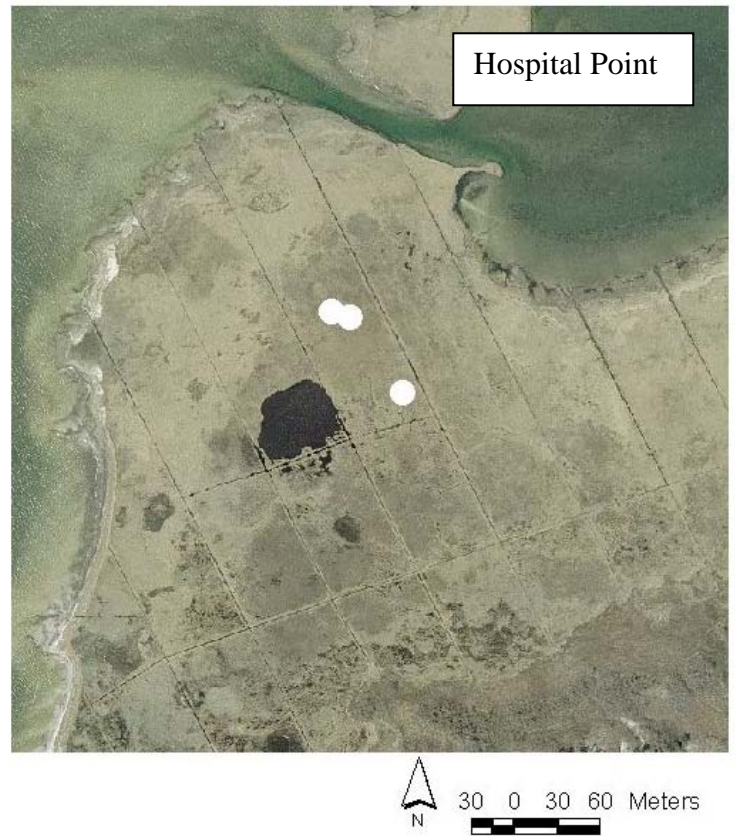


Fig. 2.2. Three study sites showing location of 3 SET stations at each site. Image Source: Digital natural color orthoimagery, 2001, New York State Office for Technology.

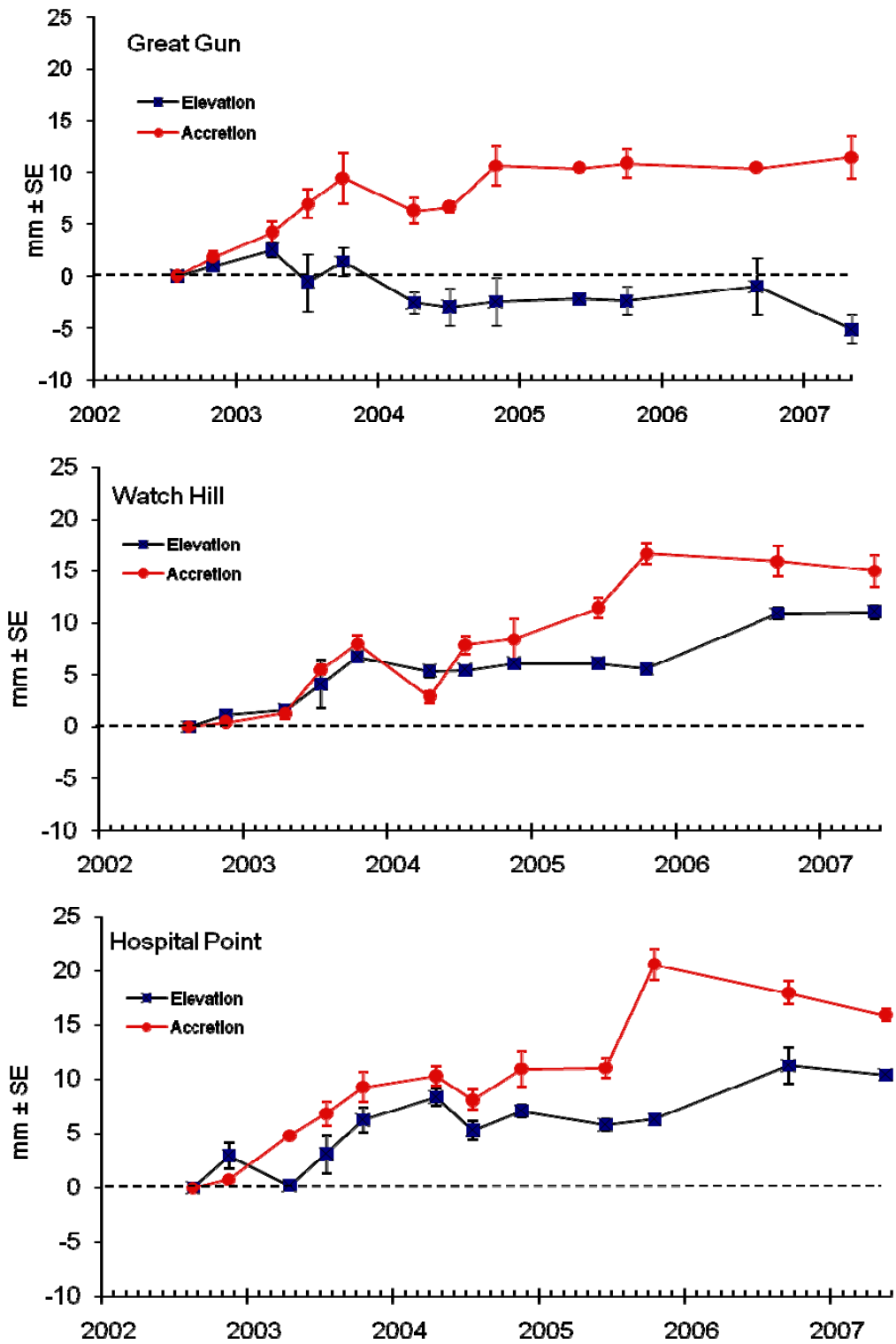


Fig. 2.3. Marsh surface elevation change and vertical accretion at three sites.

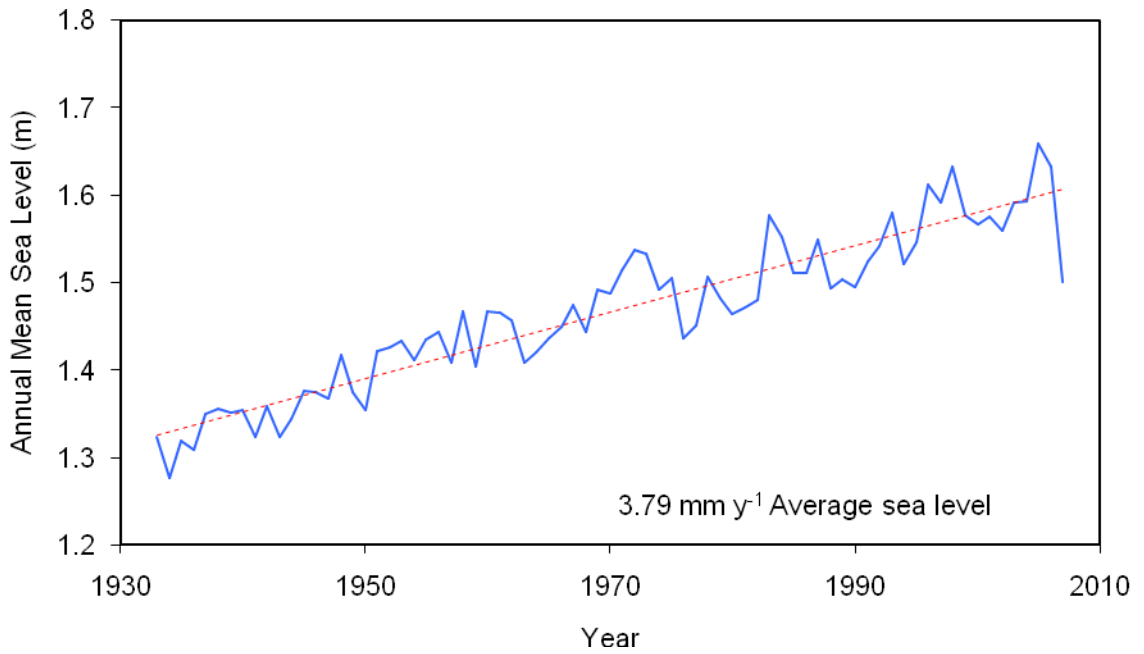


Fig. 2.4. Increase in mean annual sea level at the Sandy Hook, NJ, water level station, November 1932 to May 2007. Data source: [http://tidesandcurrents.noaa.gov/data\\_menu.shtml?stn=8531680+Sandy+Hook+%2C+NJ&type=Tide+Data&submit=Click+to+Select+Station](http://tidesandcurrents.noaa.gov/data_menu.shtml?stn=8531680+Sandy+Hook+%2C+NJ&type=Tide+Data&submit=Click+to+Select+Station)



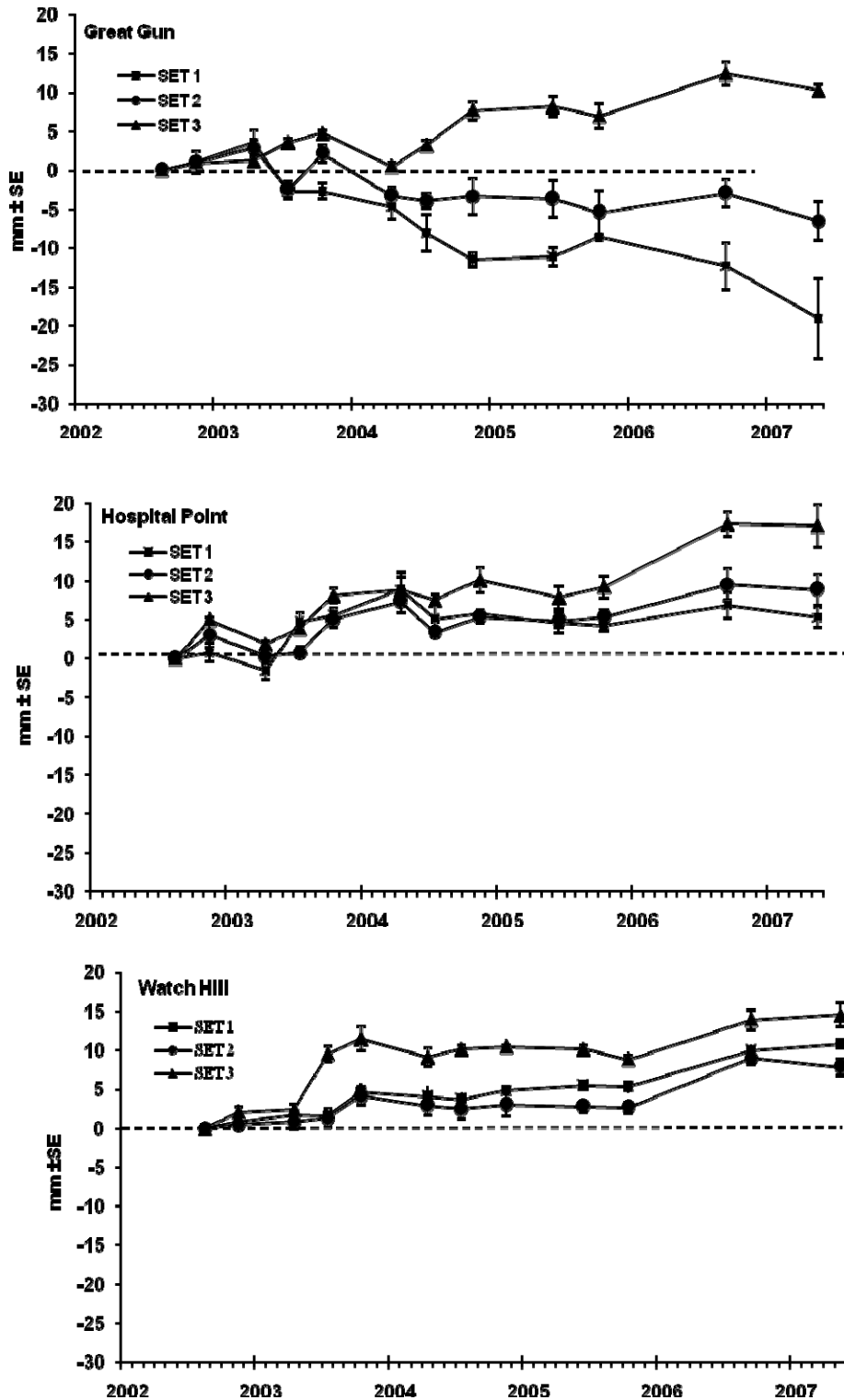


Fig. 2.5. Marsh surface elevation change showing the individual replicate SETs at each study site.

Table 2.1. Location and depth below the marsh surface of the SET benchmark pipes and dominant vegetation of each SET station. Key to vegetation: Sp, *Spartina patens*; SAS, *Spartina alterniflora* short form (<50cm tall); Sa, *Spartina alterniflora* (>1m).

| SET SITE              | UTM-North | UTM-East | Depth of Benchmark Pipe (m) | Vegetation of SET plot |
|-----------------------|-----------|----------|-----------------------------|------------------------|
| <b>Great Gun</b>      |           |          |                             |                        |
| GG_01                 | 686878    | 4514323  | 15.8                        | Sa                     |
| GG_02                 | 686867    | 4514338  | 17.1                        | Sa                     |
| GG_03                 | 686849    | 4514361  | 17.1                        | Sas, Sp                |
| <b>Hospital Point</b> |           |          |                             |                        |
| HP_01                 | 677998    | 4510928  | 17.1                        | Sp, Sas                |
| HP_02                 | 678011    | 4510924  | 14.6                        | Sas                    |
| HP_03                 | 678047    | 4510871  | 15.8                        | Sp, Sas                |
| <b>Watch Hill</b>     |           |          |                             |                        |
| WH_01                 | 670420    | 4506793  | 15.5                        | Sas                    |
| WH_02                 | 670442    | 4506825  | 15.5                        | Sas                    |
| WH_03                 | 670483    | 4506826  | 15.5                        | Sas                    |

Table 2.2. Marsh surface elevation change and rate of vertical accretion for the three study sites. Rates (i.e., regression coefficients or slopes) are based on linear regression, and compared by ANOVA and multiple contrast test.

| Site           | Elevation Change<br>mm y <sup>-1</sup> (SE) | Accretion<br>mm y <sup>-1</sup> (SE) |
|----------------|---|--------------------------------------|
| Great Gun      | -1.05 (0.98)                                | 2.12 (0.32)                          |
| Hospital Point | 2.04 (0.35)                                 | 3.76 (0.36)                          |
| Watch Hill     | 2.08 (0.35)                                 | 3.67 (0.32)                          |
|                | Compare elevation change<br>among sites:    | Compare accretion among<br>sites:    |
|                | GG<HP $p<0.0001$                            | GG<HP $p=0.0007$                     |
|                | GG<WH $p<0.0001$                            | GG<WH $p=0.0014$                     |
|                | HP=WH $p=0.9557$                            | HP=WH $p=0.8517$                     |

Table 2.3. Rate of rise in relative sea level from several NOAA water level stations in the vicinity of Fire Island. Long-term rates are derived from a linear regression of average annual mean sea level. Data source: [http://www.co-ops.nos.noaa.gov/data\\_res.html](http://www.co-ops.nos.noaa.gov/data_res.html); <http://pagebang.com/cgi/nph-proxy.cgi/111011A/http/waterdata.usgs.gov/ny/nwis?program=nwis&office=ny>

| <b>NOAA Water Level Station</b>   | <b>Relative Sea Level Rise mm y<sup>-1</sup> (SE)</b> |
|---|---|
| <u>Sandy Hook, NJ (#8531680-NOAA station)</u><br>1933 – May 2007        | 3.79 (0.17)   |
| <u>Battery, NY (#8518750-NOAA station)</u><br>1905 – May 2007           | 3.14 (0.13)   |
| <u>Montauk, NY(#8510560-NOAA station)</u><br>1947 – May 2007            | 2.52 (0.25)   |
| <u>Lindenhurst, NY (#01309225-USGS station)</u><br>July 2002 – May 2007 | -9.84 (11.2)  |

## CHAPTER 3

### Radiometric Dating and Analysis of Marsh Sediment Cores

Contributing Authors: John W. King and Peter G. Appleby

---

#### INTRODUCTION

Radiometric dating of salt marsh cores has proven to be a useful method of determining marsh accretion rates in response to sea level rise, storms, inlet changes, and other factors (e.g., Orson and Howes 1992, Roman et al. 1997, Donnelly and Bertness 2001). Marsh core data provide accretion rate estimates on a time scale of decades to centuries and a useful historical context for the shorter-term (months to years) SET data.

#### METHODS

##### Field Methods

At each of the three study sites, three salt marsh cores were obtained (Figure 3.1) adjacent to the SET locations (Table 2.1). All core sites were located in *Spartina alterniflora* and/or *Spartina patens* vegetation, and at least 5 m from tidal creeks, ditches, pools, or bay fronts.

The cores were obtained using 10 cm diameter polycarbonate tubing. A 10-cm circle was cut through the fresh, fibrous surface marsh vegetation (without compaction) to a depth of 20 cm using a very sharp serrated knife. The core tube was inserted to 20 cm in depth, a doubled "2 x 8" piece of wood was placed on top of the tube and a sledge hammer was used to pound the tube to a depth of 70-95 cm. A post-hole digger was then used to excavate a hole to the bottom of the tube, a hoe was inserted to the bottom of the hole, placed under the core tube, and used to lift the core out of the hole. The core tube was then capped at the bottom, cut down to the marsh surface sediment level, capped at the top, and transported to the laboratory. The hole was filled with the excavated sediment.

##### Core Logging Methods

All nine cores were split in half lengthwise using a core splitter at the University of Rhode Island's Graduate School of Oceanography. The split cores were then digitally imaged and the images analyzed for RGB (red-green-blue) color using the URI GeoTek core logging system. The magnetic susceptibility, a measure of magnetic concentration,

and the GRAPE (gamma ray attenuation porosity evaluator), a measure of wet bulk density were also measured at a 1 cm interval on the GeoTek logging system.

The organic carbon content of the cores was determined by the loss-on-ignition method (Dean 1974) at core intervals of approximately 2.5cm.

### **Radiometric Dating Methods**

Samples from three cores (GG1-2, HP2-1 and WH3-2) were analyzed for  $^{210}\text{Pb}$ ,  $^{226}\text{Ra}$ ,  $^{137}\text{Cs}$  and  $^{241}\text{Am}$  by direct gamma assay in the Liverpool University Environmental Radioactivity Laboratory, using Ortec HPGe GWL series well-type coaxial low background intrinsic germanium detectors (Appleby et al. 1986).  $^{210}\text{Pb}$  was determined via its gamma emissions at 46.5keV, and  $^{226}\text{Ra}$  by the 295keV and 352keV  $\gamma$ -rays emitted by its daughter isotope  $^{214}\text{Pb}$  following 3 weeks storage in sealed containers to allow radioactive equilibration.  $^{137}\text{Cs}$  and  $^{241}\text{Am}$  were measured by their emissions at 662keV and 59.5 keV respectively. The absolute efficiencies of the detectors were determined using calibrated sources and sediment samples of known activity. Corrections were made for the effect of self absorption of low energy  $\gamma$ -rays within the sample (Appleby et al. 1992).

## **RESULTS**

### **Core Logging and Lithology**

The GeoTek core logging data and images from three Watch Hill site cores and three Hospital Point cores are shown in Figs. 3.2 - 3.4 and Figs. 3.5 – 3.7, respectively. All of the cores from these two sites had a 40 - 50 cm thick surficial layer of marsh peat underlain by sand. No sand layers were observed within the peat. GeoTek core logging data and images from three Great Gun cores are shown in Figs. 3.8 - 3.10, with a 45 - 48 cm thick surficial layer of marsh peat underlain by sand. All Great Gun cores contained an approximately 7 cm silt layer from 13 - 20 cm in depth within the surficial peat.

The results of the loss-on-ignition analysis are shown in Figs. 3.11 - 3.13. All three sites were similar in having little organic matter in the underlying sands. The Watch Hill and Hospital Point sites (Figs. 3.11 - 3.12) had relatively high organic contents in the overlying marsh peats that tended to increase toward the surface. The Watch Hill site marsh peat (Fig. 3.11) had a slightly higher organic content than the Hospital Point marsh peats (Fig. 3.12). The Great Gun site (Fig. 3.13) marsh peats had comparable or higher organic contents than the other sites except for the upper 20 cm.

## Radiometric Dating

Detailed radiometric results for each core are given in Tables 3.1-3.3 and shown graphically in Figs. 3.14 - 3.18. Mean  $^{226}\text{Ra}$  (supported  $^{210}\text{Pb}$ ) concentrations in the three cores were relatively uniform, ranging from 18-22  $\text{Bq kg}^{-1}$ . Table 3.4 provides a number of parameters characterizing the records of fallout radionuclides in each core, including the maximum unsupported  $^{210}\text{Pb}$  concentration, the unsupported  $^{210}\text{Pb}$  inventory, the mean  $^{210}\text{Pb}$  flux required to sustain this inventory, and the  $^{137}\text{Cs}$  inventory. Also shown are the mean atmospheric fluxes for New England. The cores all have a good record of  $^{210}\text{Pb}$  fallout, with  $^{210}\text{Pb}$  inventories comparable to the value supported by the atmospheric flux. The moderately higher value at WH3-2 could indicate a certain degree of sediment focusing at this site. In common with most estuarine sites, the  $^{137}\text{Cs}$  inventories are substantially lower than the fallout value. The deficiency (when normalized against  $^{210}\text{Pb}$ ) varies from a little over 50% at GG1-2 to more than 80% at WH3-2. In spite of these losses, the cores all contained a well-defined subsurface peak in  $^{137}\text{Cs}$  activity that could be used to identify the depths of sediments recording the 1963 fallout maximum.

Radiometric dates for each core were calculated using the CRS (Constant Rate of Supply)  $^{210}\text{Pb}$  dating model (Appleby et al. 1978), and compared with stratigraphic dates determined from the  $^{137}\text{Cs}$  record. Use of the CIC (Constant Initial Concentration) model was precluded by the non-monotonic nature of most of the  $^{210}\text{Pb}$  profiles. Best chronologies for each core were determined using the procedures described in Appleby and Oldfield (1983) and Appleby (2001). The results of these calculations are given in Tables 3.5 - 3.7 and Figs. 3.15, 3.17, and 3.19. Table 3.8 summarizes the mean post-1963 sedimentation rates in each core determined from the  $^{137}\text{Cs}$  record.

### *Core GG1-2*

#### Lead-210 Activity

Total  $^{210}\text{Pb}$  activity in this core reaches equilibrium with the supporting  $^{226}\text{Ra}$  at a depth of about 25 cm (Fig. 3.14a). Unsupported  $^{210}\text{Pb}$  activity varies irregularly with depth, with significant non-monotonic features between 4-9 cm, and 12-19 cm. It is evident from Fig. 3.14b, plotting unsupported  $^{210}\text{Pb}$  together with dry bulk density, that the irregularities in the  $^{210}\text{Pb}$  record in this core coincide with layers of dense sediment and are most probably related to the geomorphic events causing these layers. The relatively abrupt disappearance of unsupported  $^{210}\text{Pb}$  below 25 cm suggests that there may be another such event at the base of the  $^{210}\text{Pb}$  record, though in this case it does not appear to be associated with a change in sediment density.

#### Artificial Fallout Radionuclides

The  $^{137}\text{Cs}$  activity versus depth record in this core (Fig. 3.14c) has a well resolved peak between 9-12 cm that almost certainly records the 1963 fallout maximum from the atmospheric testing of nuclear weapons. This interpretation is supported by the presence of traces of  $^{241}\text{Am}$  at the same depth as the  $^{137}\text{Cs}$  peak, though it should be noted that there are substantial  $^{137}\text{Cs}$  concentrations down to 17 cm, with a small secondary peak at

14.5 cm, and that the profile below 12 cm may have been distorted by the event associated with formation of the dense layer below 12 cm.

#### Core Chronology

Fig. 3.15 shows  $^{210}\text{Pb}$  dates calculated using the CRS model, together with the 1963 depth determined from the  $^{137}\text{Cs}$  record. The  $^{210}\text{Pb}$  results place 1963 at a depth of ca. 12.5 cm, a little below the depth indicated by the  $^{137}\text{Cs}$  record. Calculations using the 1963  $^{137}\text{Cs}$  date as a reference level indicate that the post-1963  $^{210}\text{Pb}$  supply rate is quite close to the atmospheric flux, but that the pre-1963 supply rate was substantially higher. The most likely cause was excessive deposition at this site during events associated with the formation of the dense layer below 12 cm. Uncertainties in the nature of these events and their impact on the  $^{210}\text{Pb}$  record make the dating of these older sections highly problematic. Depending on the model used, the section from 10.5-26.5 cm could span anywhere between 30-140 years. Taking a relatively conservative approach, the 90% equilibrium depth (1928, corresponding to 74 years deposition) occurs at between 19-23 cm. A composite chronology was calculated using the intermediate depth as a reference point. The results, plotted in Fig. 3.15 and given in detail in Table 3.5, indicate episodes of rapid accumulation in the early 1950s and early 1980s, possibly due to particular storm events. The mean post-1963 accumulation rate is calculated to be  $0.082 \text{ g cm}^{-2} \text{ y}^{-1}$  (or  $0.27 \text{ cm y}^{-1}$ ). The long-term mean accumulation rate during the 20<sup>th</sup> century is calculated to be  $0.092 \text{ g cm}^{-2} \text{ y}^{-1}$  (or  $0.28 \text{ cm y}^{-1}$ ).

#### **Core HP2-1**

##### Lead-210 Activity

Total  $^{210}\text{Pb}$  activity in the Hospital Point core reaches equilibrium with the supporting  $^{226}\text{Ra}$  at a depth of about 30 cm (Fig. 3.16a). Unsupported  $^{210}\text{Pb}$  activity (Fig. 3.16b) again varies irregularly with depth, though less so than at GG1-2. There is however a significant non-monotonic feature between 8-11 cm, and some smaller irregularities in the deeper sections. Unlike GG1-2, the feature at 8-11 cm is not associated with any major change in the sediment density.

##### Artificial Fallout Radionuclides

The  $^{137}\text{Cs}$  activity versus depth record in this core (Fig. 3.16c) has a well resolved peak between 15-18 cm that probably records the 1963 fallout maximum from the atmospheric testing of nuclear weapons, though in this case  $^{241}\text{Am}$  concentrations were below limits of detection. As at GG1-2, there is a small secondary peak 4 cm below the main peak. Since it is not clear whether this feature is a true record of atmospheric fallout, or the result of sedimentological process, there must remain some uncertainty as to the precise 1963 depth.

##### Core Chronology

Fig. 3.17 shows  $^{210}\text{Pb}$  dates calculated using the CRS model, together with the 1963 depth determined from the  $^{137}\text{Cs}$  record. The  $^{210}\text{Pb}$  results place 1963 at a depth of between 10.5 cm, in this case significantly above the 1963 depth indicated by the  $^{137}\text{Cs}$  record. Calculations using the 1963  $^{137}\text{Cs}$  date as a reference level indicate that the post-1963  $^{210}\text{Pb}$  supply rate is again quite close to the atmospheric flux, but that the pre-1963



supply rate was substantially lower, possibly due to losses from the early part of the sediment record during episodes of erosion. Corrected  $^{210}\text{Pb}$  dates were calculated using the  $^{137}\text{Cs}$  date as a reference point. The results, plotted in Fig. 3.17 and given in detail in Table 3.6, indicate an episode of very rapid accumulation in the mid 1970s. The mean post-1963 accumulation rate is calculated to be  $0.066 \text{ g cm}^{-2} \text{ y}^{-1}$  (or  $0.42 \text{ cm y}^{-1}$ ). The higher volumetric rate compared to GG1-2, in spite of the lower dry mass rate, reflects the lower dry bulk density of the sediments at this site. The long-term mean accumulation rate during the 20<sup>th</sup> century is calculated to be  $0.046 \text{ g cm}^{-2} \text{ y}^{-1}$  (or  $0.29 \text{ cm y}^{-1}$ ).

### ***Core WH3-2***

#### Lead-210 Activity

Total  $^{210}\text{Pb}$  activity in this core reaches equilibrium with the supporting  $^{226}\text{Ra}$  at a depth of about 17 cm (Fig. 3.18a). The graph of unsupported  $^{210}\text{Pb}$  activity versus depth (Fig. 3.18b) again deviates significantly from a simple exponential relation, indicating non-uniform accumulation. Although there are none of the major non-monotonic features seen at the other two sites, there is a relatively abrupt change in gradient at around 11 cm that may indicate a systematic increase in accumulation rates.

#### Artificial Fallout Radionuclides

The  $^{137}\text{Cs}$  activity versus depth record in this core (Fig. 3.18c) has a well resolved peak between 7-10 cm. The presence of traces of  $^{241}\text{Am}$  at the same depth shows that this feature almost certainly records the 1963 fallout maximum from the atmospheric testing of nuclear weapons.

#### Core Chronology

Fig. 3.19 shows  $^{210}\text{Pb}$  dates calculated using the CRS model, together with the 1963 depth determined from the  $^{137}\text{Cs}$  record. The  $^{210}\text{Pb}$  results place 1963 at a depth of about 7.3 cm, a little above the 1963 depth determined from the  $^{137}\text{Cs}$  record. Corrected  $^{210}\text{Pb}$  dates were calculated using the 1963  $^{137}\text{Cs}$  date as a reference level. The results, plotted in Figure 3.19, and given in detail in Table 3.7, suggest a significant increase in sedimentation rates in the early 1960s, but that values since then have remained relatively constant. This increase was associated with a moderate increase in the  $^{210}\text{Pb}$  flux, suggesting that it may be partly due to a change in the pattern of sediment accumulation. The mean post-1963 accumulation rate is calculated to be  $0.045 \text{ g cm}^{-2} \text{ y}^{-1}$  (or  $0.22 \text{ cm y}^{-1}$ ), and the long-term (20<sup>th</sup> century) mean to be  $0.034 \text{ g cm}^{-2} \text{ y}^{-1}$  (or  $0.17 \text{ cm y}^{-1}$ ). Although there is no clear evidence of any major disruptions (e.g. due to storm events), the relatively abrupt disappearance of  $^{210}\text{Pb}$  below 13 cm could be due to such an event, and in view of this, dates from the deeper sections of the core should be regarded with some caution. If there is evidence of such event from other sources, the  $^{210}\text{Pb}$  record would place it at a depth of between 14-17 cm, and date it to the early 1930s.

## **Timing of Changes in Organic Content**

The Great Gun site (Fig. 3.20) marsh peats have comparable or higher organic contents than the other sites (except for the upper 20 cm) until approximately the mid-1930s, when they decrease abruptly with a change in lithology to clay-silt. The clay-silt persists until the mid-1960s, until marsh peat of significantly lower organic content is again deposited. Deposition of marsh peat of lower organic content than both the Hospital Point and Watch Hill sites persists until the present.

## **DISCUSSION**

### **Initiation of Peat Deposition**

An estimate of the date of initiation of peat deposition can be obtained by extrapolation of the lowest reliable linear sedimentation rate obtained in each age model to the base of the peat layer. For example, the lowest reliable linear sedimentation rate estimate for the Great Gun site is 0.18 cm/year at 20.5 cm in depth. The estimated age of initial peat deposition obtained by extrapolating this sedimentation rate to the base of the peat at 50 cm is 1766 AD. Note that compaction of the peat is not taken into account by this approach, and this is therefore a minimum age estimate. This approach yields an estimated age of initial peat deposition at Hospital Point of 1778 AD, and an estimated age of initial peat deposition at Watch Hill of 1589 AD. Given the inherent errors in the age model, the estimates for Great Gun and Hospital Point are equivalent, whereas the age of initial peat deposition at Watch Hill is distinctly older than the other sites.

### **Impact of Storms and Inlet Changes**

The initiation of peat deposition at Great Gun and Hospital Point appears to coincide in age with the opening of the adjacent Halletts' (1788) and Smiths' (1773) inlets, respectively (Fig. 1.3). Perhaps creation of these inlets resulted in a flood tidal delta or sand platform in the bay that was suitable for *Spartina alterniflora* establishment, as well as enabling a bay salinity condition that was conducive to *Spartina* growth. The role of inlets and barrier island overwash events in the bayward transport of sediment, flood tide delta formation, and marsh development has been described in detail (e.g., Fisher and Simpson 1979, Leatherman 1979, Leatherman and Allen 1985, Roman and Nordstrom 1988, Donnelly et al. 2004).

A clear correlation exists between the opening of the Moriches Inlet in 1931 (Fig. 1.3) and the abrupt termination of peat deposition and initiation of silt deposition at Great Gun. Based on chronology for core GG 1-2, the year 1930 is estimated at about 20.5 cm depth and the input of inorganic sediment is clearly noted (Figs. 3.13 and 3.20). The variation of tidal range within the study area (Figure 1.2) provides a probable explanation for observed change in lithology. It is likely that the tidal range increased substantially at Great Gun with the opening of the new inlet. This increase in tidal range would inundate

the site and perhaps change the depositional environment from *Spartina* marsh to tidal flat, then with subsequent re-development of marsh to the present.

### Comparison of Accretion Rates

A comparison of vertical accretion rates obtained by the feldspar method, recent rates from  $^{210}\text{Pb}$  chronologies (between 2002-2000 AD), and the average vertical accretion post - 1963 AD estimated by  $^{137}\text{Cs}$  is shown in Table 3.9. The various methods are within reasonable agreement, but the best is observed at Great Gun, the site with the highest tidal range and highest clastic input (lowest organic carbon content).

### LITERATURE CITED

Appleby P G, 2001. Chronostratigraphic techniques in recent sediments, in *Tracking Environmental Change Using Lake Sediments Volume 1: Basin Analysis, Coring, and Chronological Techniques*, (eds W M Last & J P Smol), Kluwer Academic, pp171-203.

Appleby, P.G., P.J. Nolan, D.W.Gifford, M.J.Godfrey, F.Oldfield, N.J.Anderson and R.W.Battarbee. 1986.  $^{210}\text{Pb}$  dating by low background gamma counting. *Hydrobiologia* 141: 21-27.

Appleby, P.G. and F. Oldfield. 1978. The calculation of  $^{210}\text{Pb}$  dates assuming a constant rate of supply of unsupported  $^{210}\text{Pb}$  to the sediment. *Catena* 5: 1-8.

Appleby, P.G. and F. Oldfield. 1983. The assessment of  $^{210}\text{Pb}$  data from sites with varying sediment accumulation rates. *Hydrobiologia* 103: 29-35.

Appleby, P.G., N. Richardson, and P.J. Nolan. 1992. Self-absorption corrections for well-type germanium detectors. *Nucl. Inst. & Methods B* 71: 228-233.

Dean, W. E. 1974. Determination of carbonate and organic matter in calcareous sediments and sedimentary rocks by loss on ignition: comparison with other methods. *Journal of Sedimentary Petrology* 44: 242-248.

Donnelly, J.P., and M.D. Bertness. 2001. Rapid shoreward encroachment of salt marsh cordgrass in response to accelerated sea-level rise. *Proceedings of the National Academy of Sciences* 98: 14218-14223.

Donnelly, J.P., J. Butler, S. Roll, M. Wengren, and T. Webb III. 2004. A backbarrier overwash record of intense storms from Brigantine, New Jersey. *Marine Geology* 107-121.

Fisher, J.J., and E. J. Simpson. 1979. Washover and tidal sedimentation rates as environmental factors in development of a transgressive barrier shoreline. Pages 127 – 148 in *Barrier Islands from the Gulf of St. Lawrence to the Gulf of Mexico* (S.P. Leatherman, ed.). Academic Press, NY.

Leatherman, S.P. 1979. Migration of Assateague Island, Maryland, by inlet and overwash processes. *Geology* 7: 104-107.

Leatherman, S.P., and J.R. Allen, eds. 1985. *Geomorphic analysis: Fire Island Inlet to Montauk Point, Long Island, New York*. NPS Technical Report to the US Army Corps of Engineers, NY District.

Orson, R.A., and B.L. Howes. 1992. Salt marsh development studies at Waquoit Bay, Massachusetts: Influence of geomorphology on long-term plant community structure. *Estuarine, Coastal and Shelf Science* 31: 453-471.

Roman, C.T., and K.F. Nordstrom. 1988. The effect of erosion rate on vegetation patterns of an East Coast barrier island. *Estuarine, Coastal and Shelf Science* 26: 233-242.

Roman, C.T., J.A. Peck, J.R. Allen, J.W. King, and P.G. Appleby. 1997. Accretion of a New England (USA) salt marsh in response to inlet migration, storms, and sea-level rise. *Estuarine, Coastal and Shelf Science* 45: 717-727.

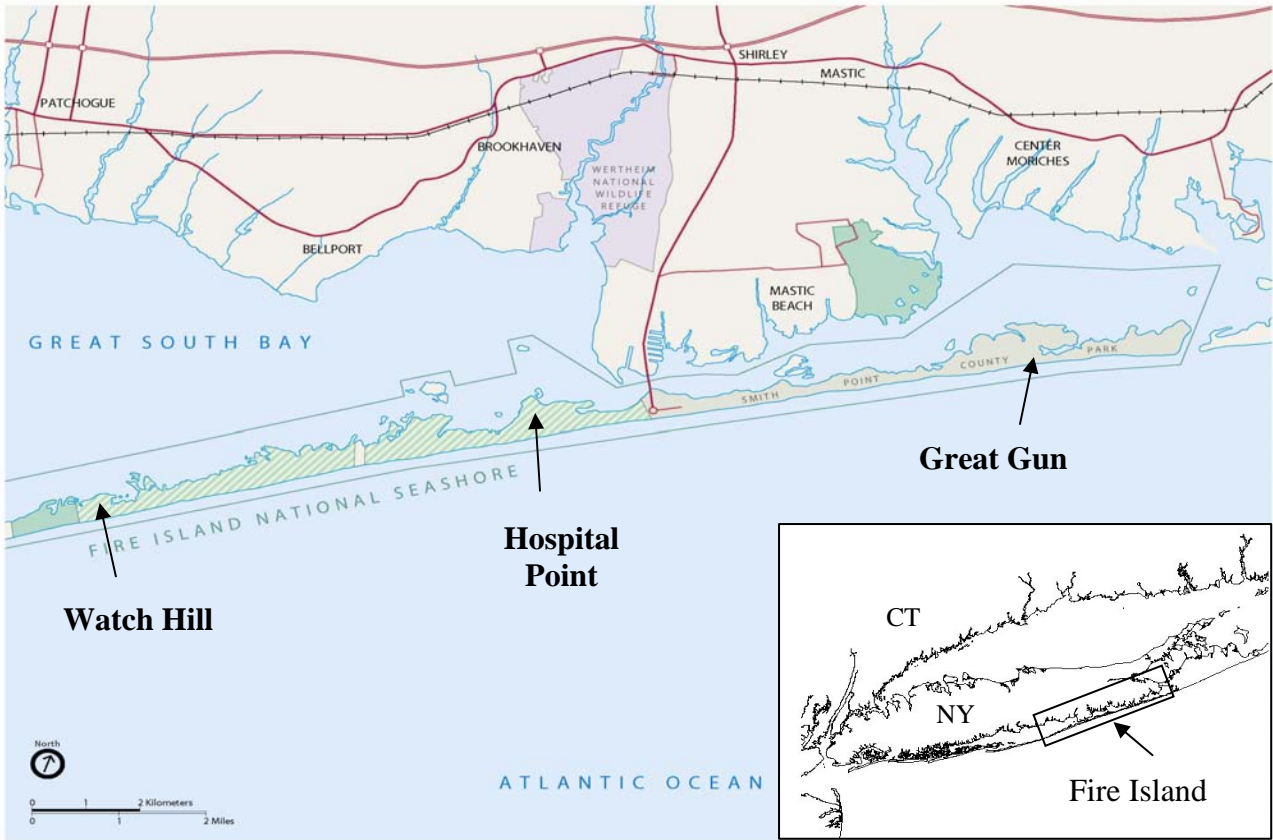


Fig. 3.1. Location of three core collection study sites.

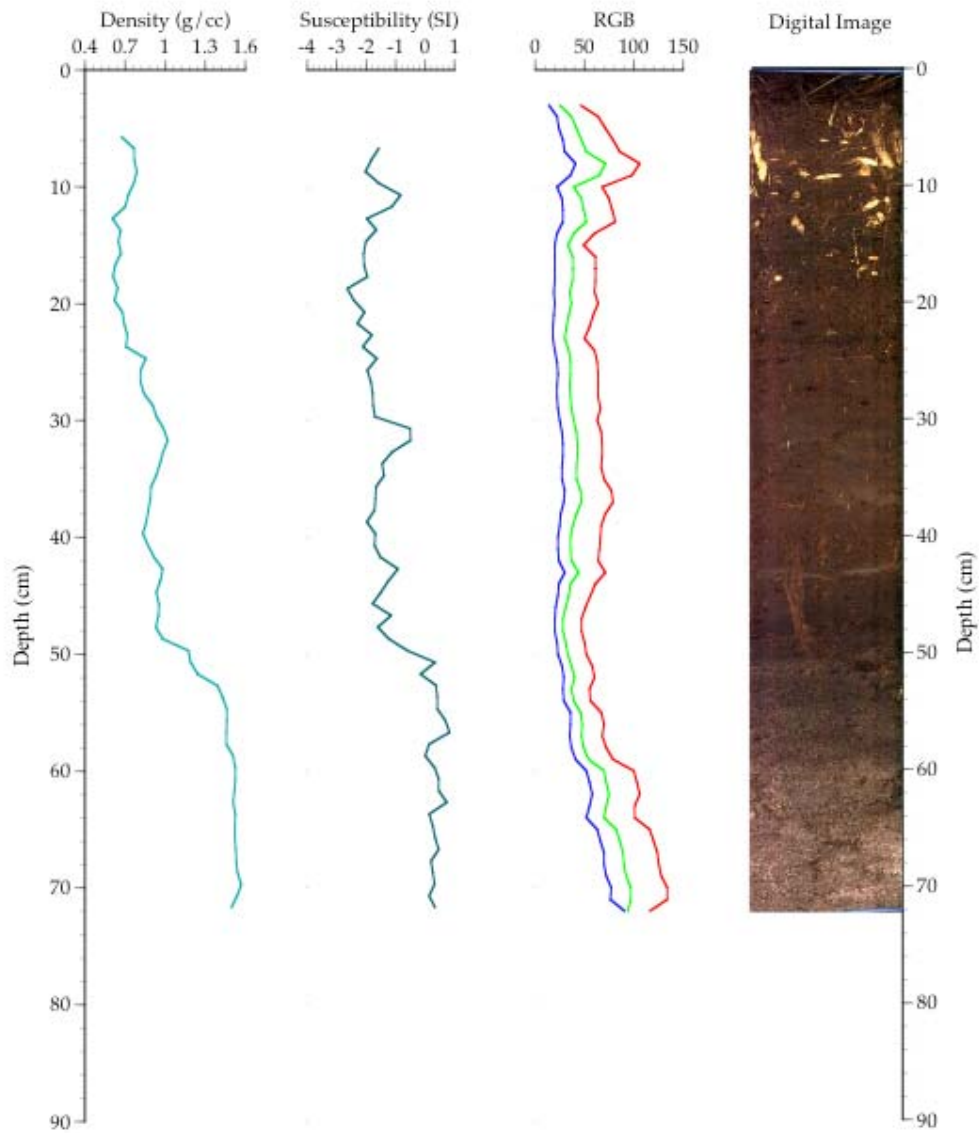


Figure 3.2 GeoTek core logging and digital image from Watch Hill, core 3-1.

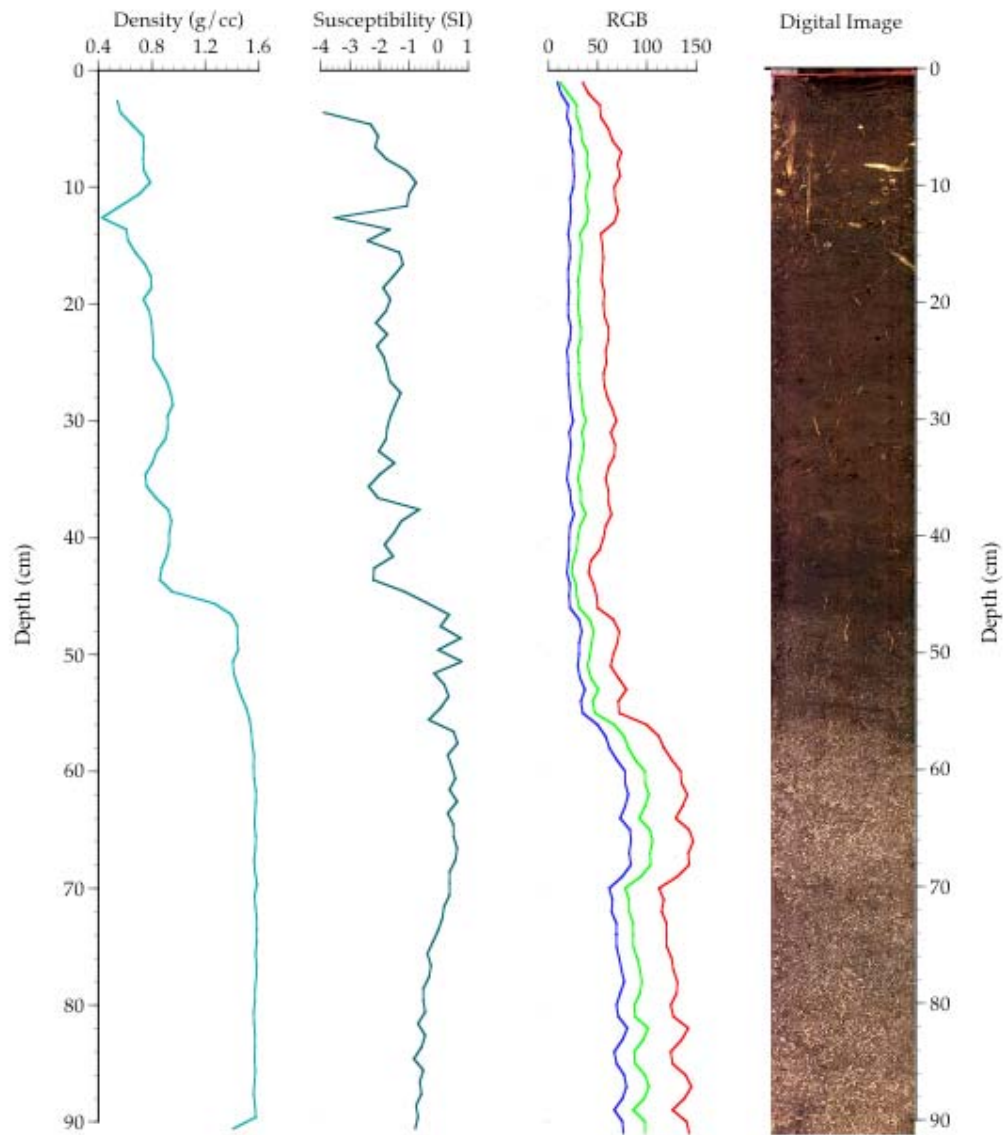


Figure 3.3. GeoTek core logging and digital image from Watch Hill, core 3-2.

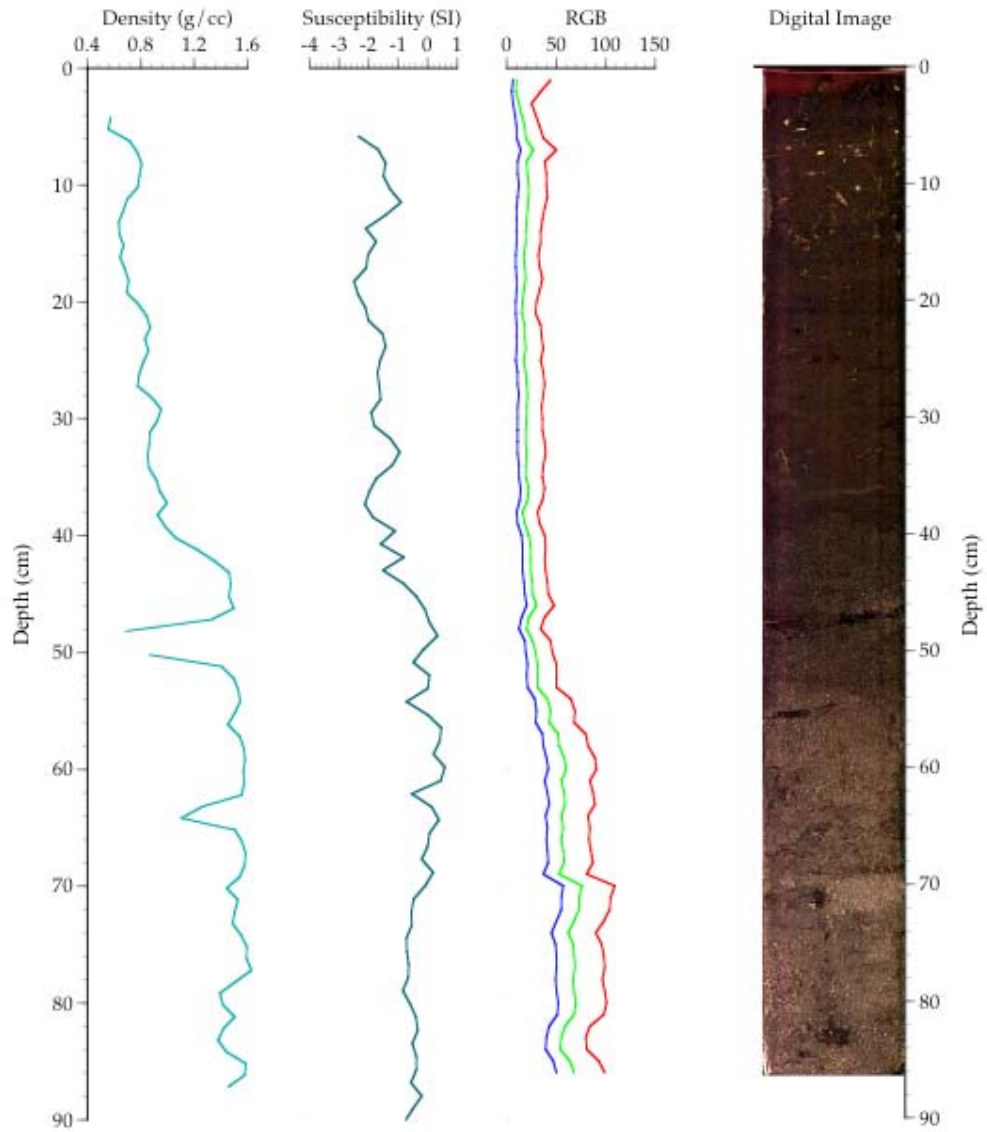


Figure 3.4. GeoTek core logging and digital image from Watch Hill, core 3-3.



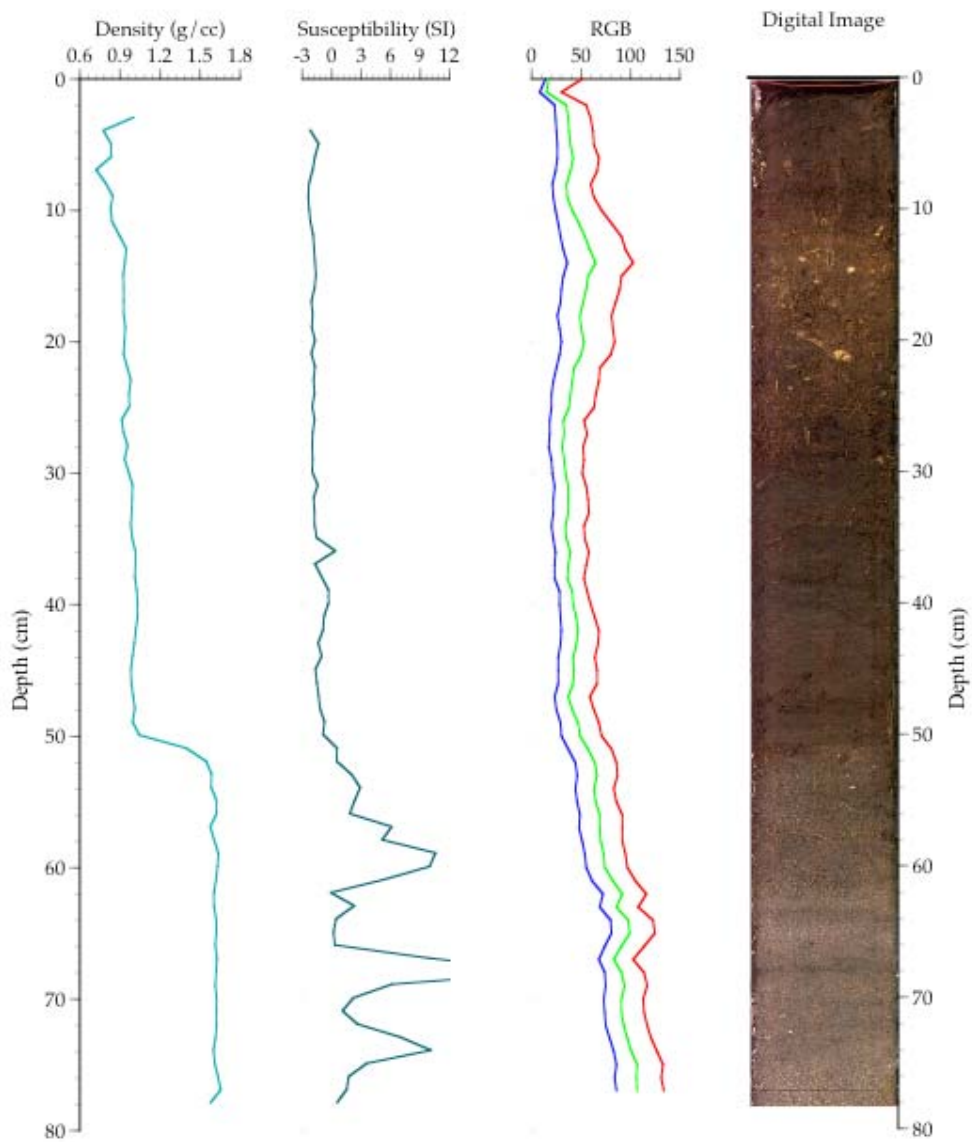


Figure 3.5. GeoTek core logging and digital image from Hospital Point, core HP 2-1.

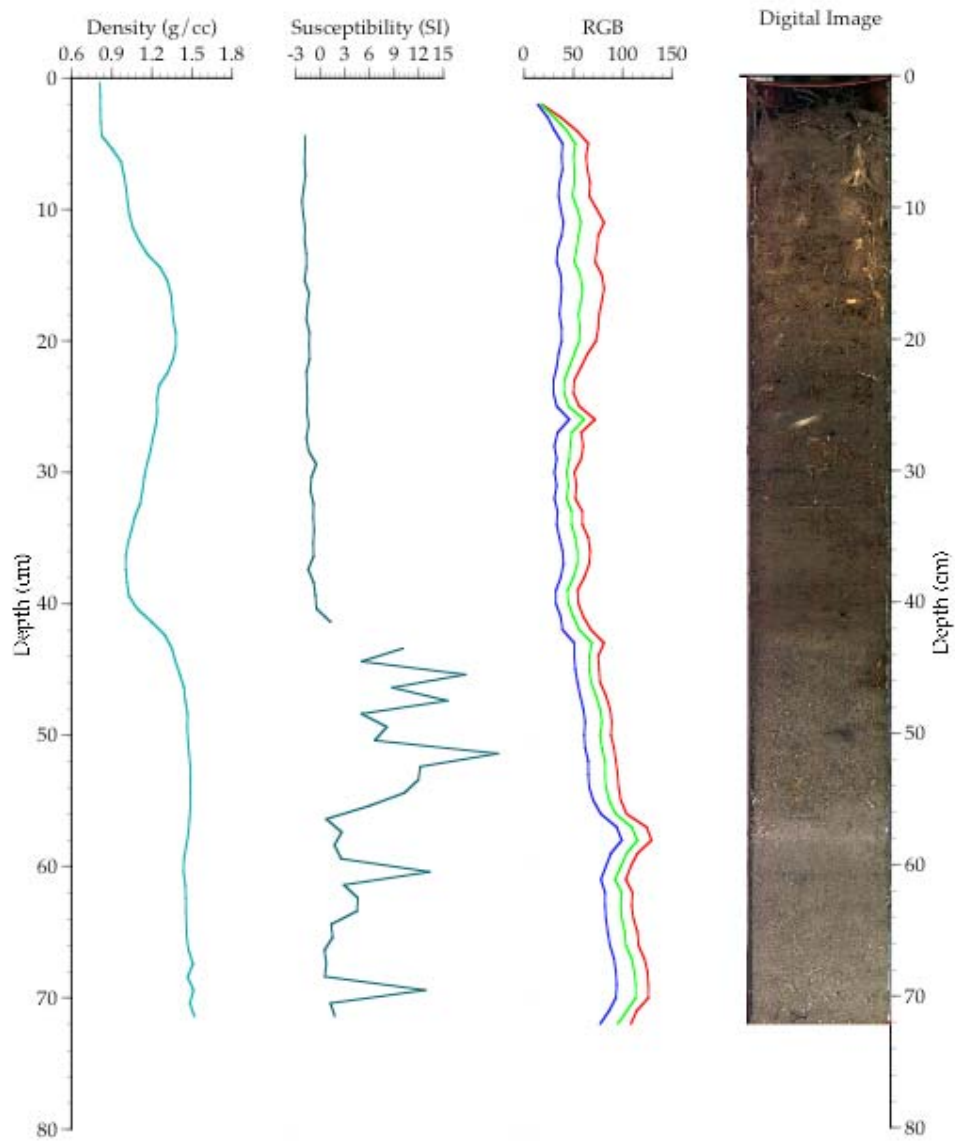


Figure 3.6. GeoTek core logging and digital image from Hospital Point, core HP 2-2.

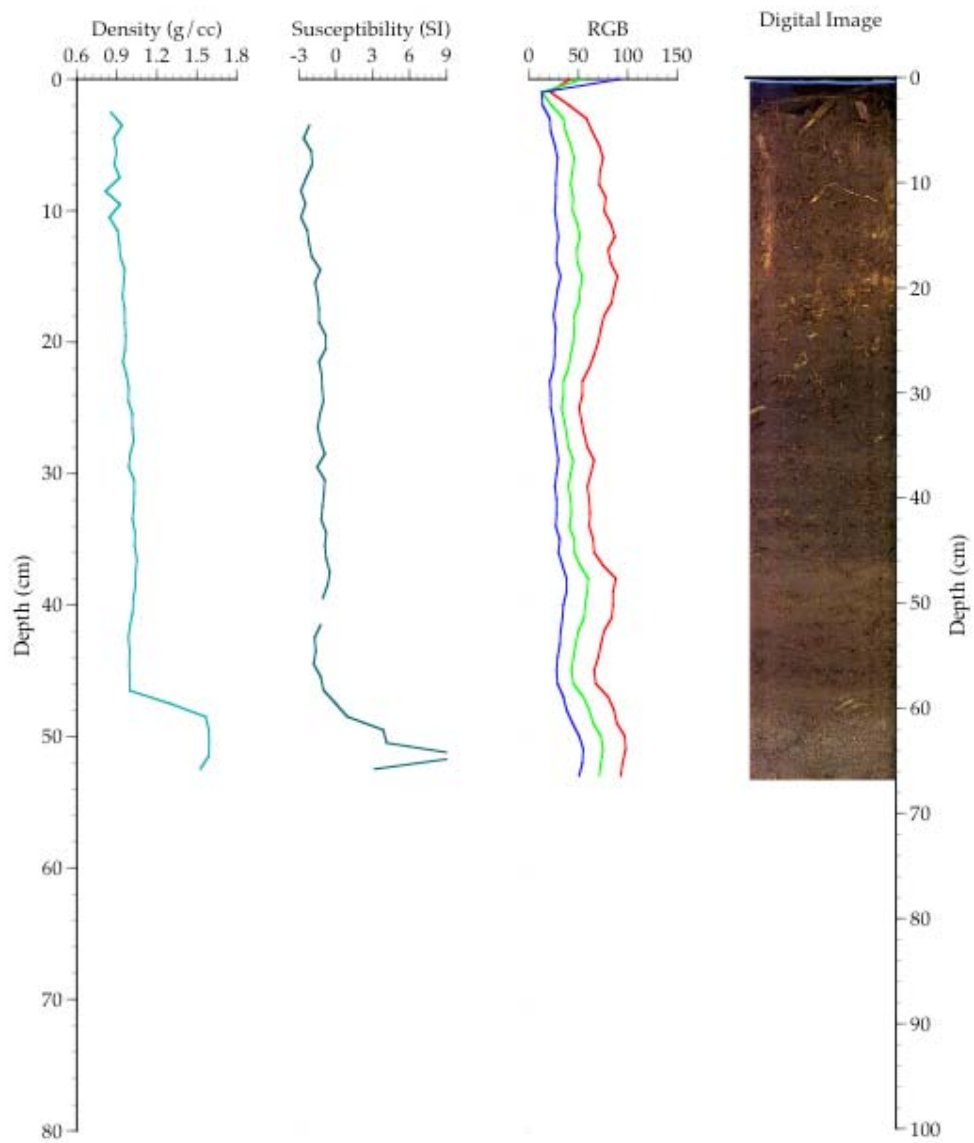


Figure 3.7. GeoTek core logging and digital image from Hospital Point, core HP 2-3.

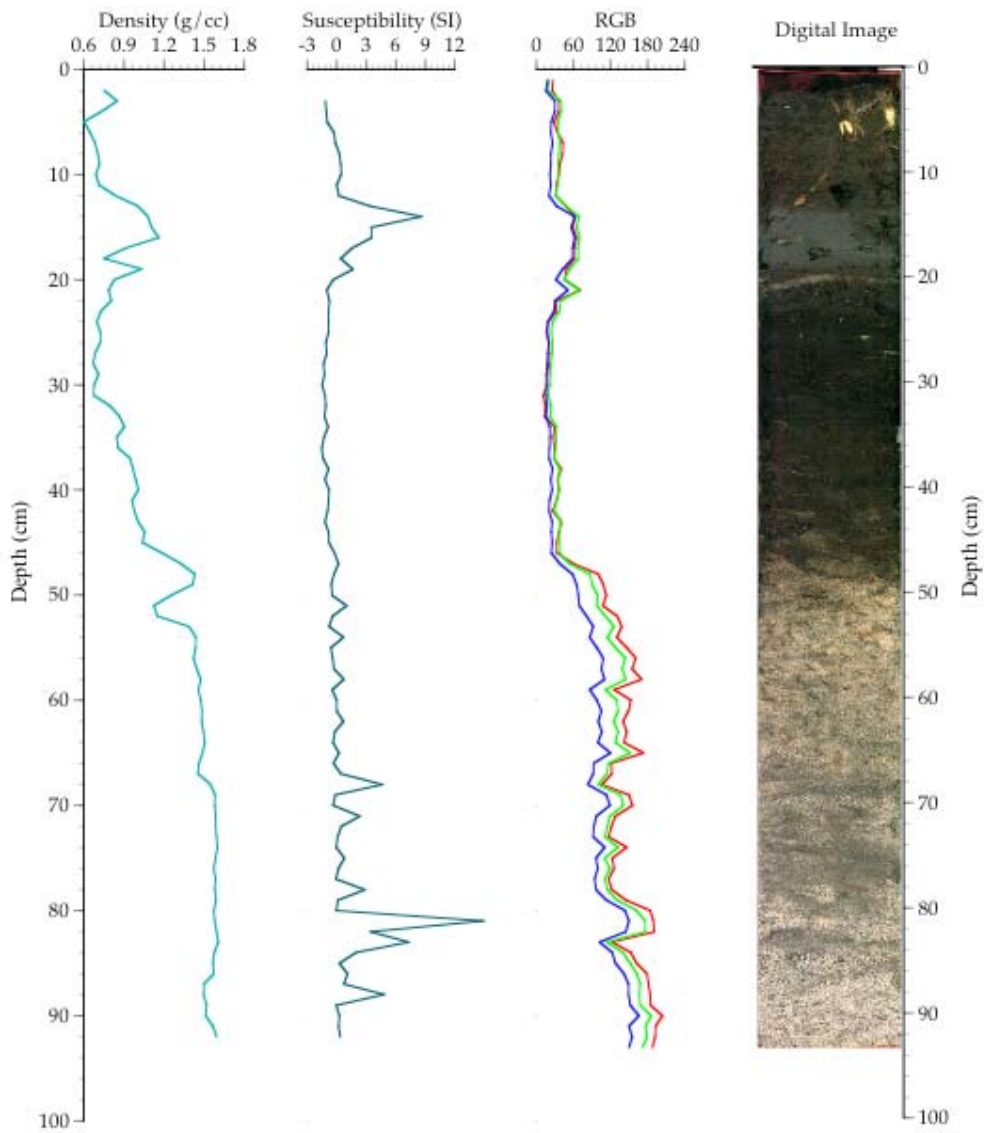


Figure 3.8. GeoTek core logging and digital image from Great Gun, core GG 1-1.

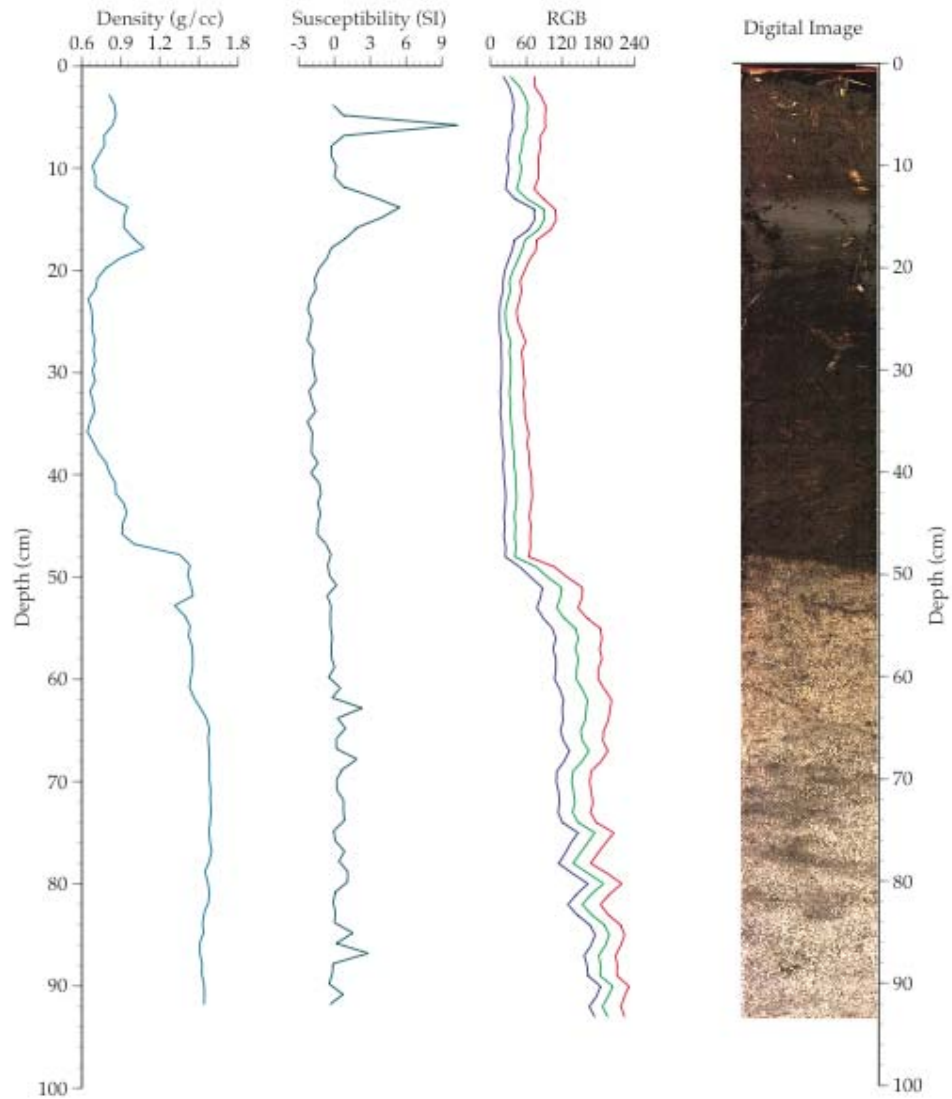


Figure 3.9. GeoTek core logging and digital image from Great Gun, core GG 1-2.

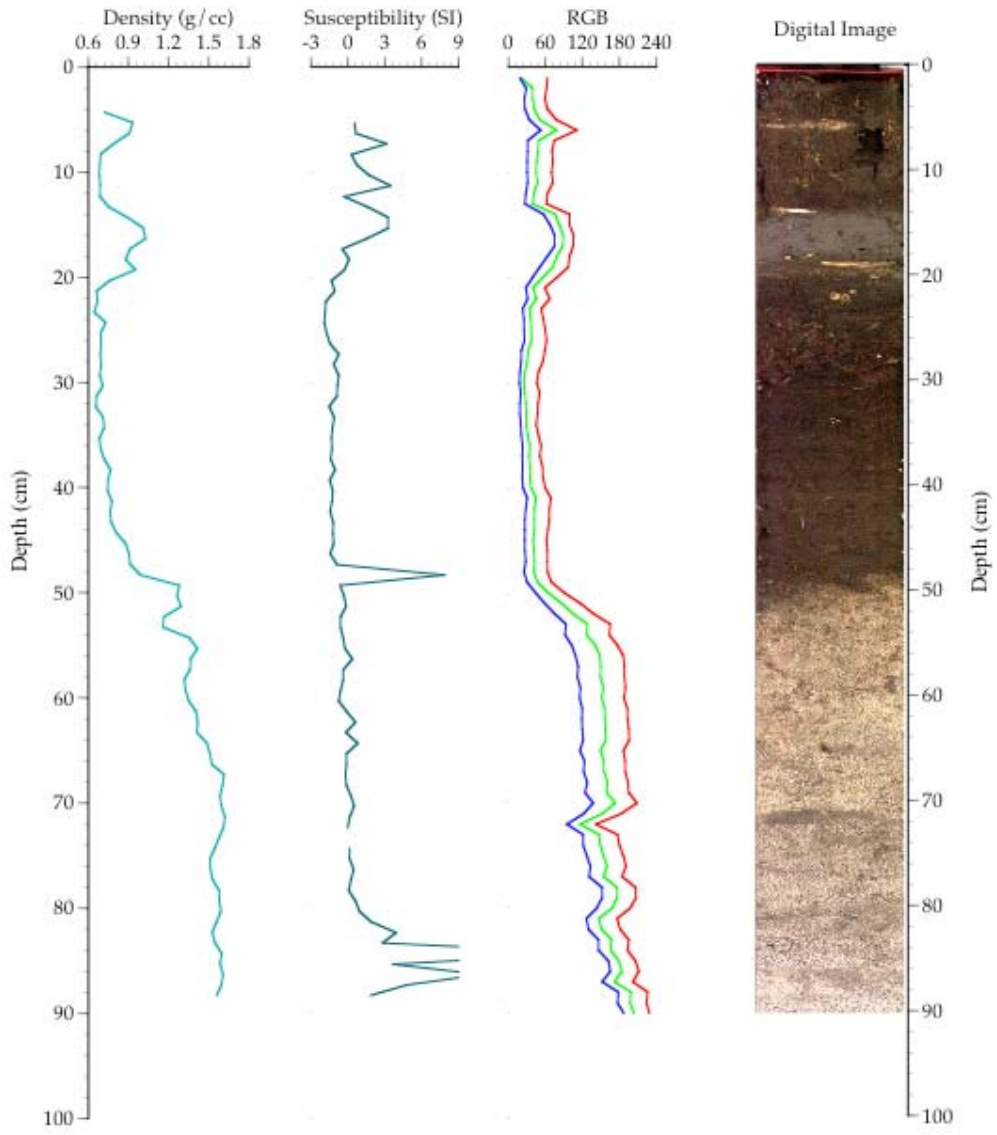


Figure 3.10. GeoTek core logging and digital image from Great Gun, core GG 1-3.

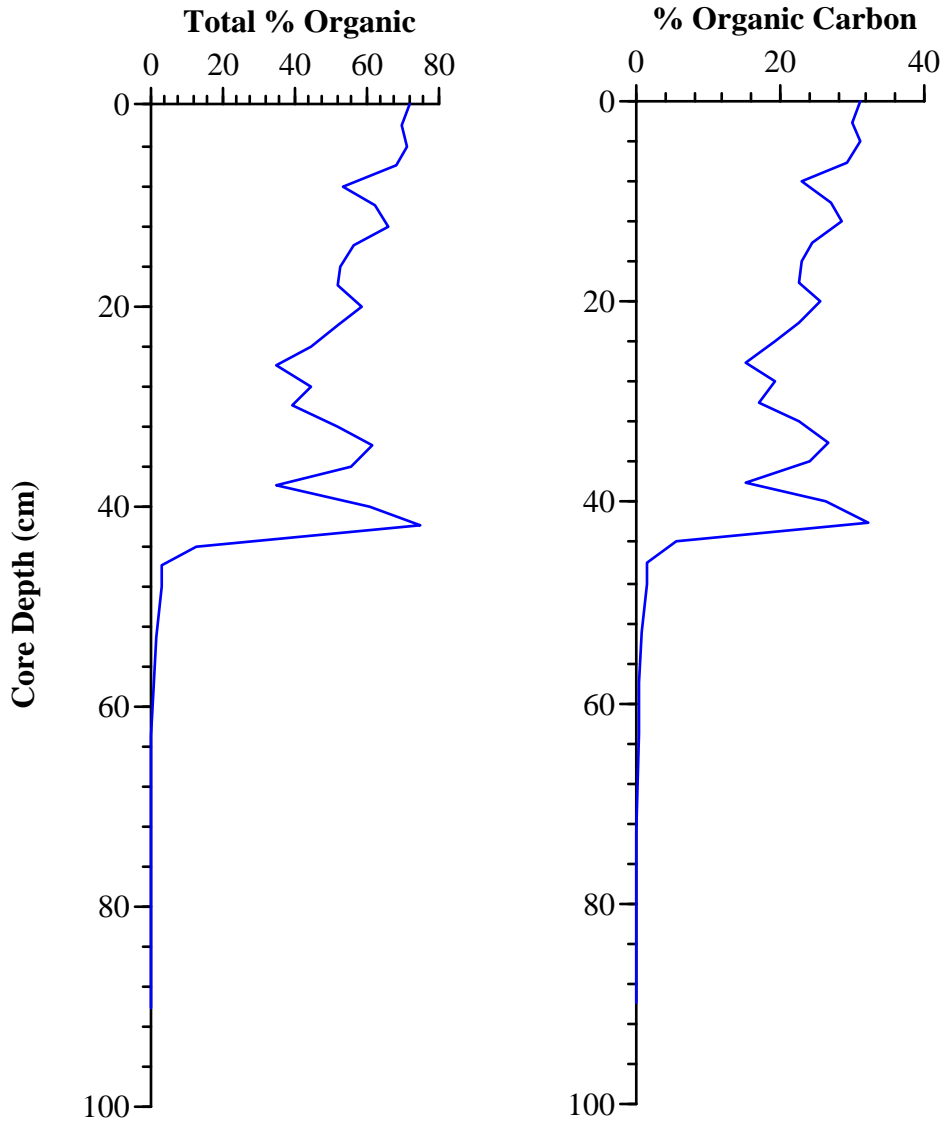


Figure 3.11. Organic content from Watch Hill, core WH 3-2.

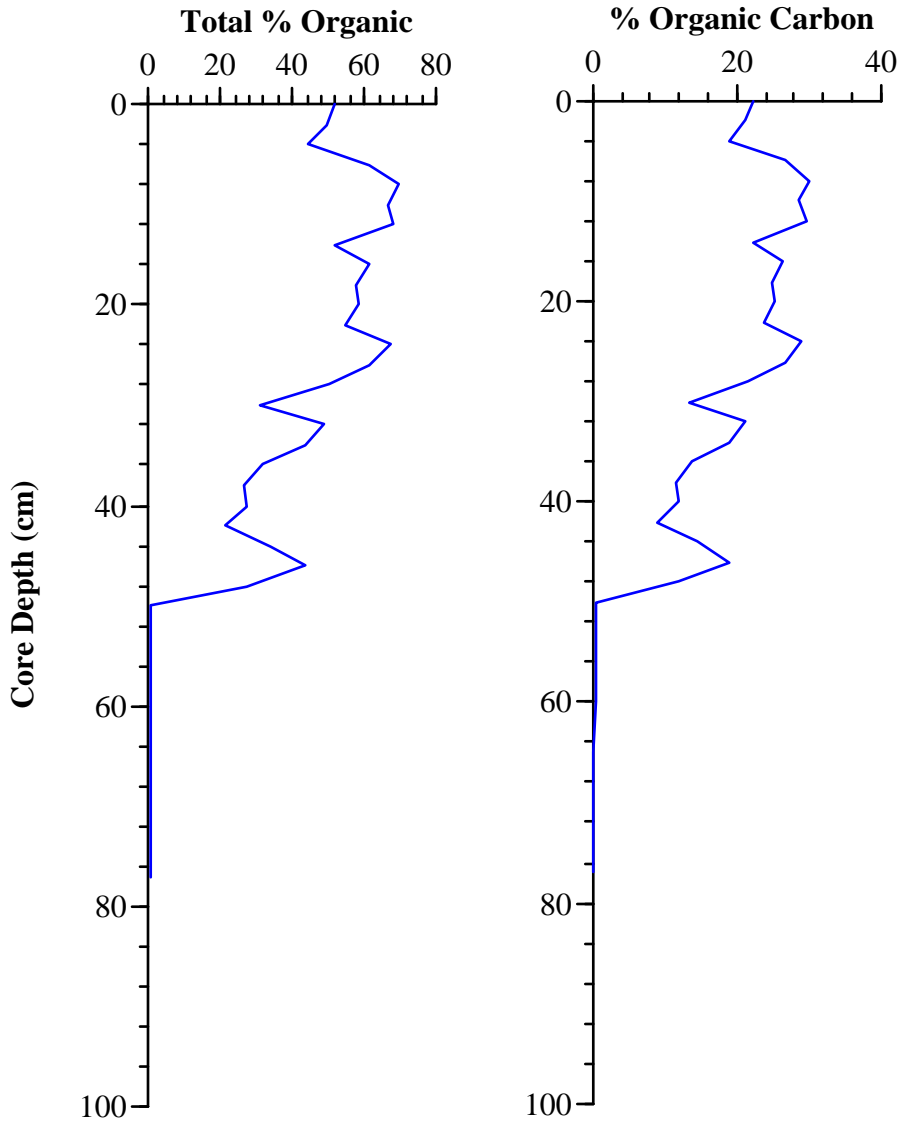


Figure 3.12. Organic content from Hospital Point, core HP 2-1.



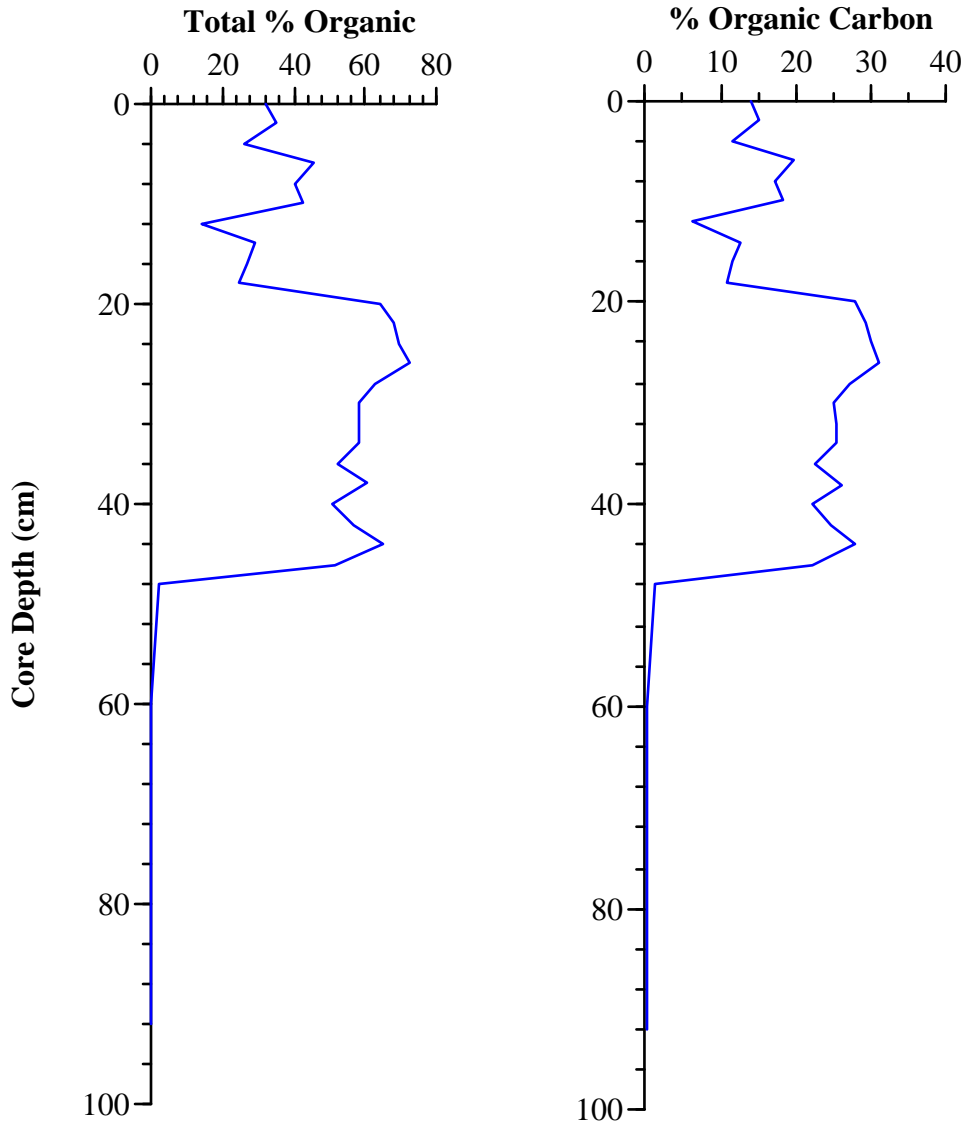


Figure 3.13. Organic content from Great Gun, core GG 1-2

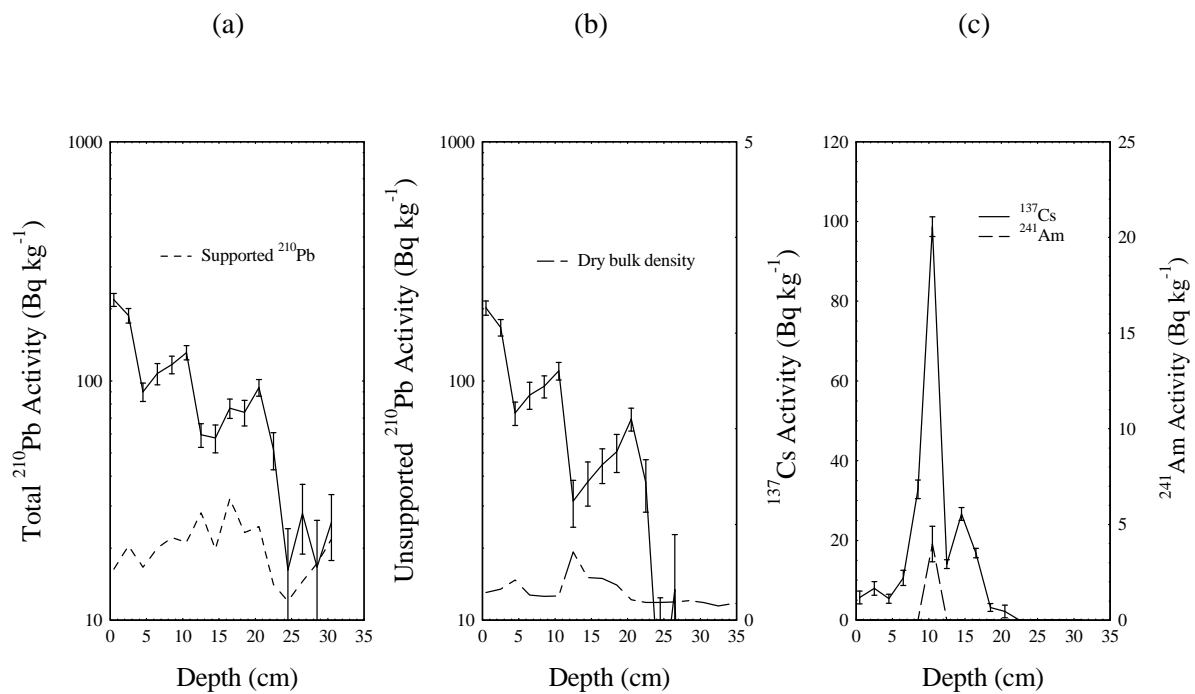


Fig. 3.14. Fallout radionuclides in Fire Island core GG1-2 showing (a) total and supported  $^{210}\text{Pb}$ , (b) unsupported  $^{210}\text{Pb}$ , (c)  $^{137}\text{Cs}$  and  $^{241}\text{Am}$  concentrations versus depth. Figure (b) also shows the dry bulk density versus depth in core GG1-2 (plotted against the second axis).

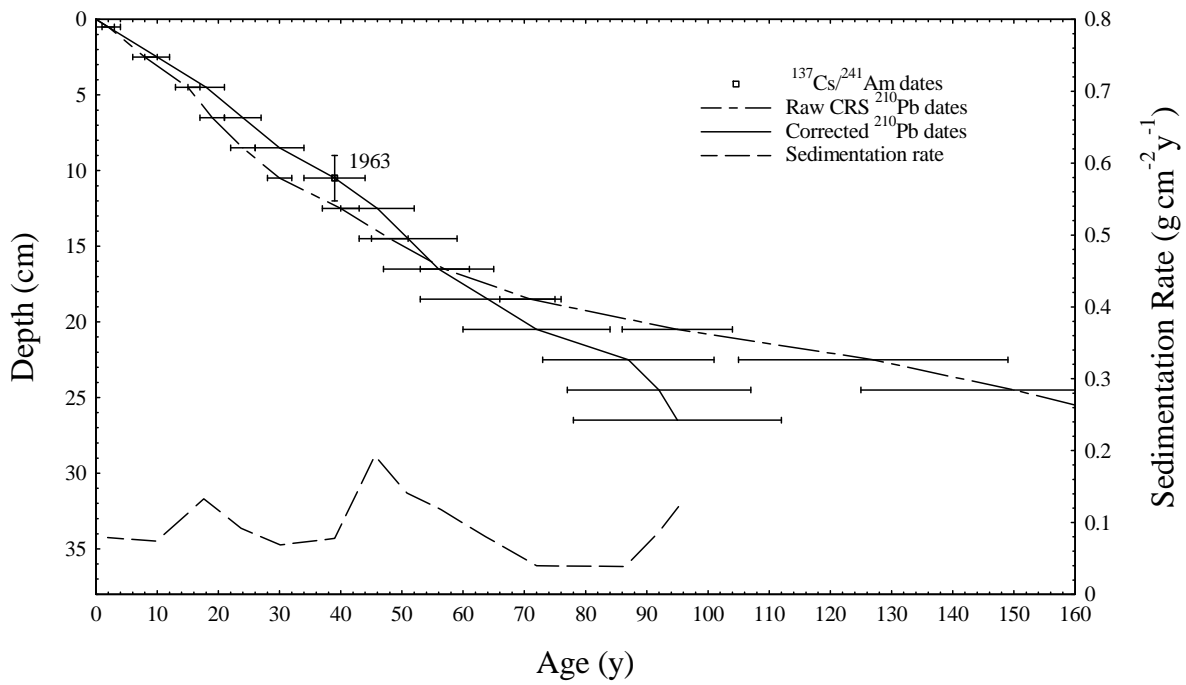


Figure 3.15 Radiometric chronology of Fire Island core GG1-2 showing the CRS model <sup>210</sup>Pb dates and the 1963 depth determined from the <sup>137</sup>Cs stratigraphy. Also shown are corrected <sup>210</sup>Pb dates and sedimentation rates calculated using the <sup>137</sup>Cs date as a reference level.

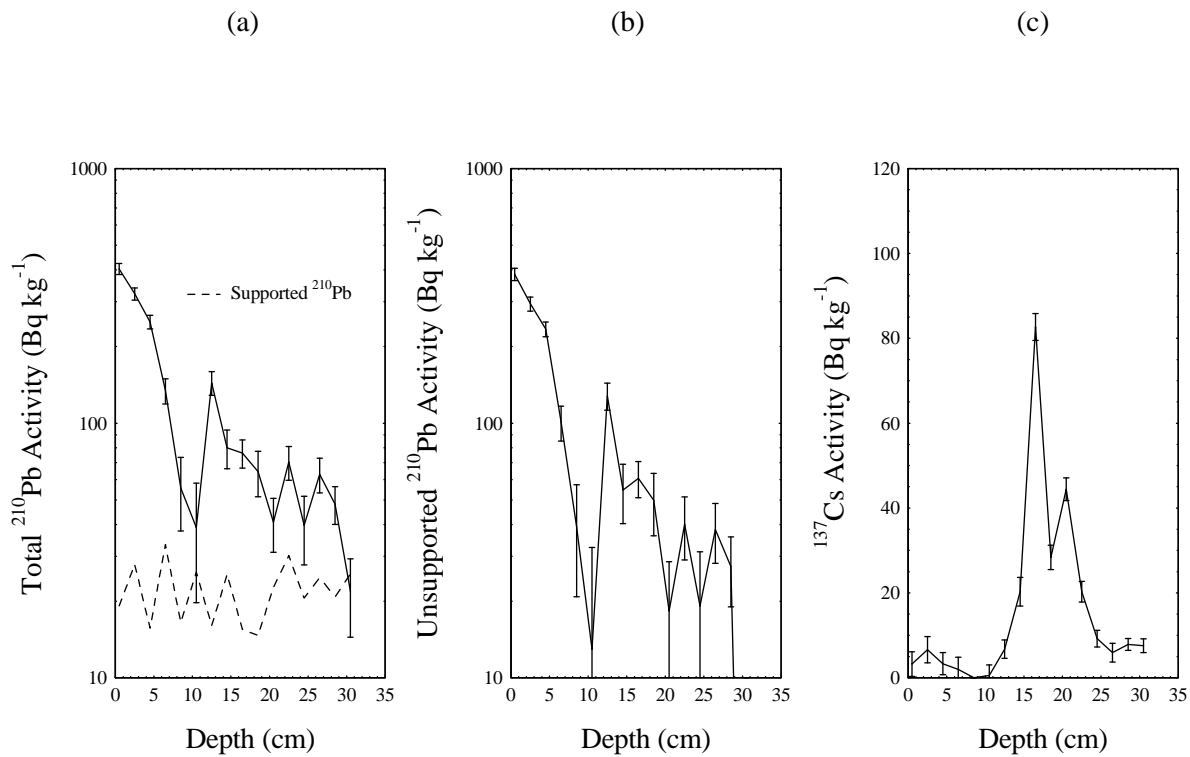


Figure 3.16. Fallout radionuclides in Fire Island core HP2-1 showing (a) total and supported  $^{210}\text{Pb}$ , (b) unsupported  $^{210}\text{Pb}$ , (c)  $^{137}\text{Cs}$  concentrations versus depth.

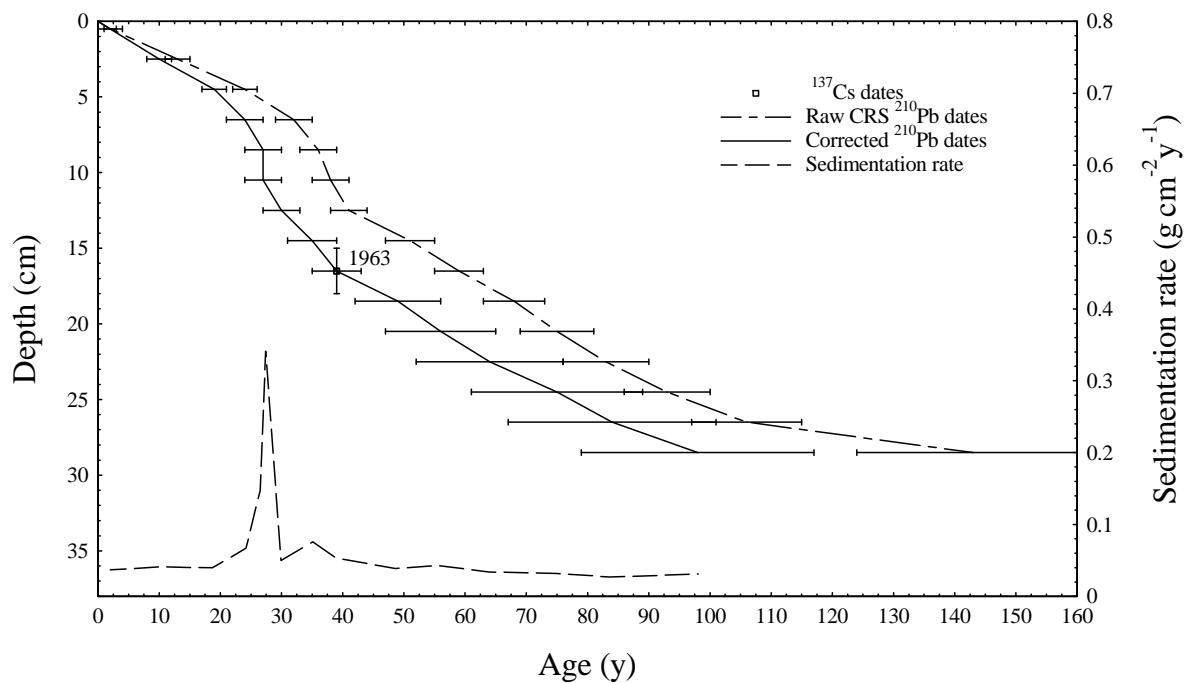


Figure 3.17. Radiometric chronology of Fire Island core HP2-1 showing the CRS model  $^{210}\text{Pb}$  dates and the 1963 depth determined from the  $^{137}\text{Cs}$  stratigraphy. Also shown are corrected  $^{210}\text{Pb}$  dates and sedimentation rates calculated using the  $^{137}\text{Cs}$  date as a reference level.

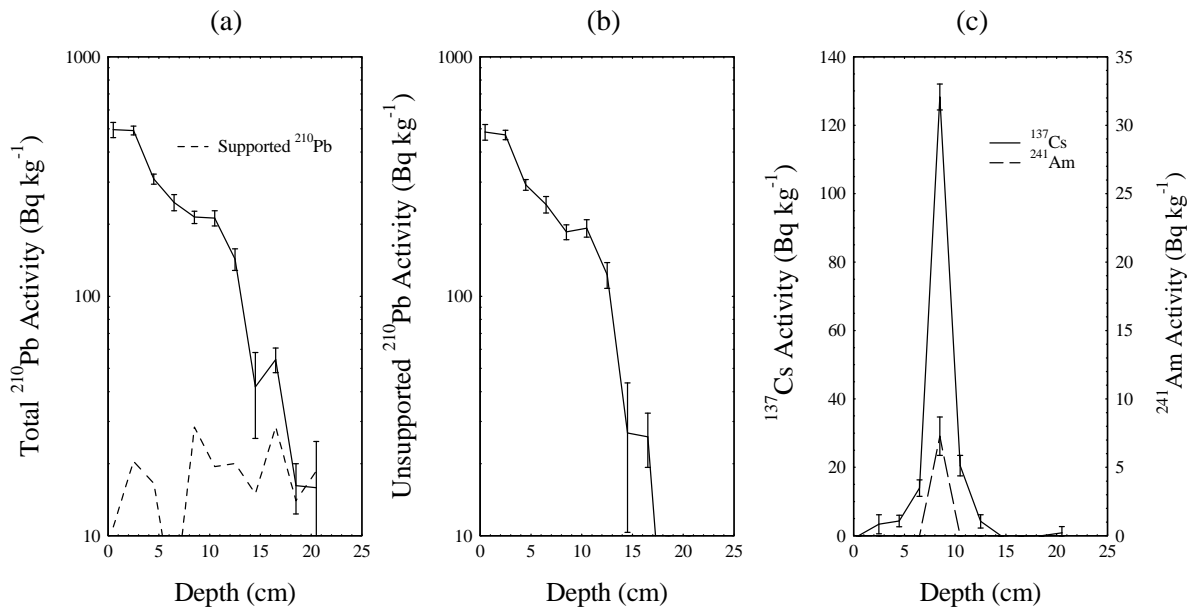


Figure 3.18. Fallout radionuclides in Fire Island core WH3-2 showing (a) total and supported  $^{210}\text{Pb}$ , (b) unsupported  $^{210}\text{Pb}$ , (c)  $^{137}\text{Cs}$  and  $^{241}\text{Am}$  concentrations versus depth.

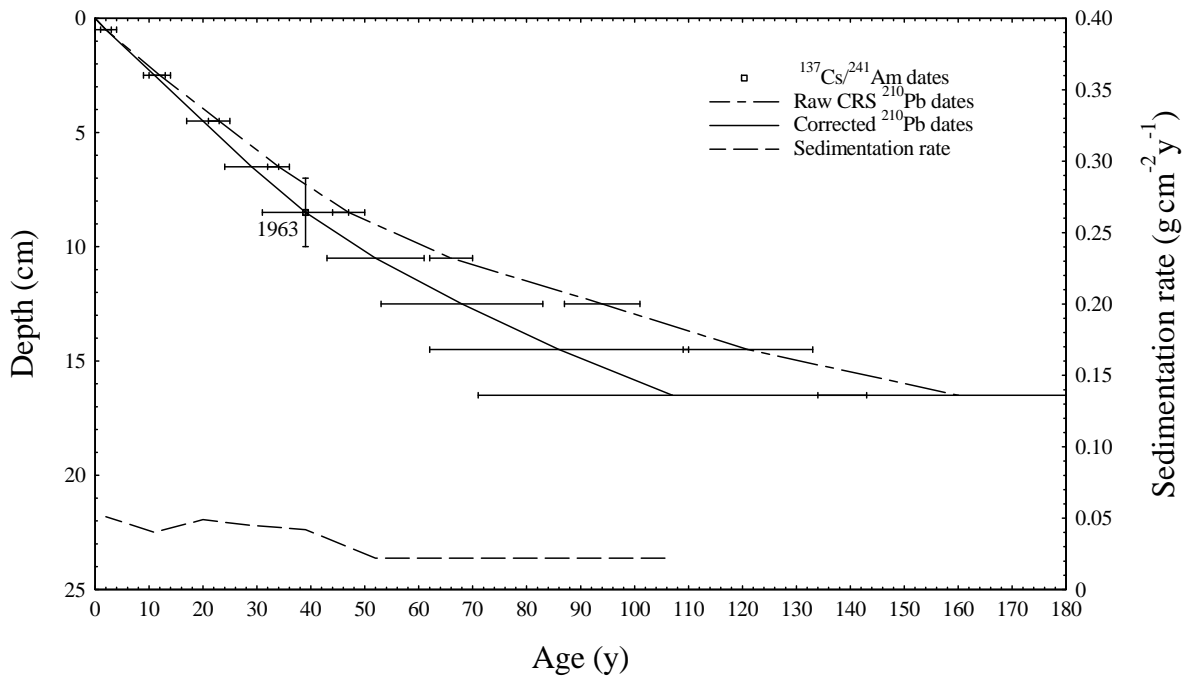


Figure 3.19 Radiometric chronology of Fire Island core WH3-2 showing the CRS model  $^{210}\text{Pb}$  dates and the 1963 depth determined from the  $^{137}\text{Cs}$  stratigraphy. Also shown are corrected  $^{210}\text{Pb}$  dates and sedimentation rates calculated using the  $^{137}\text{Cs}$  date as a reference level.

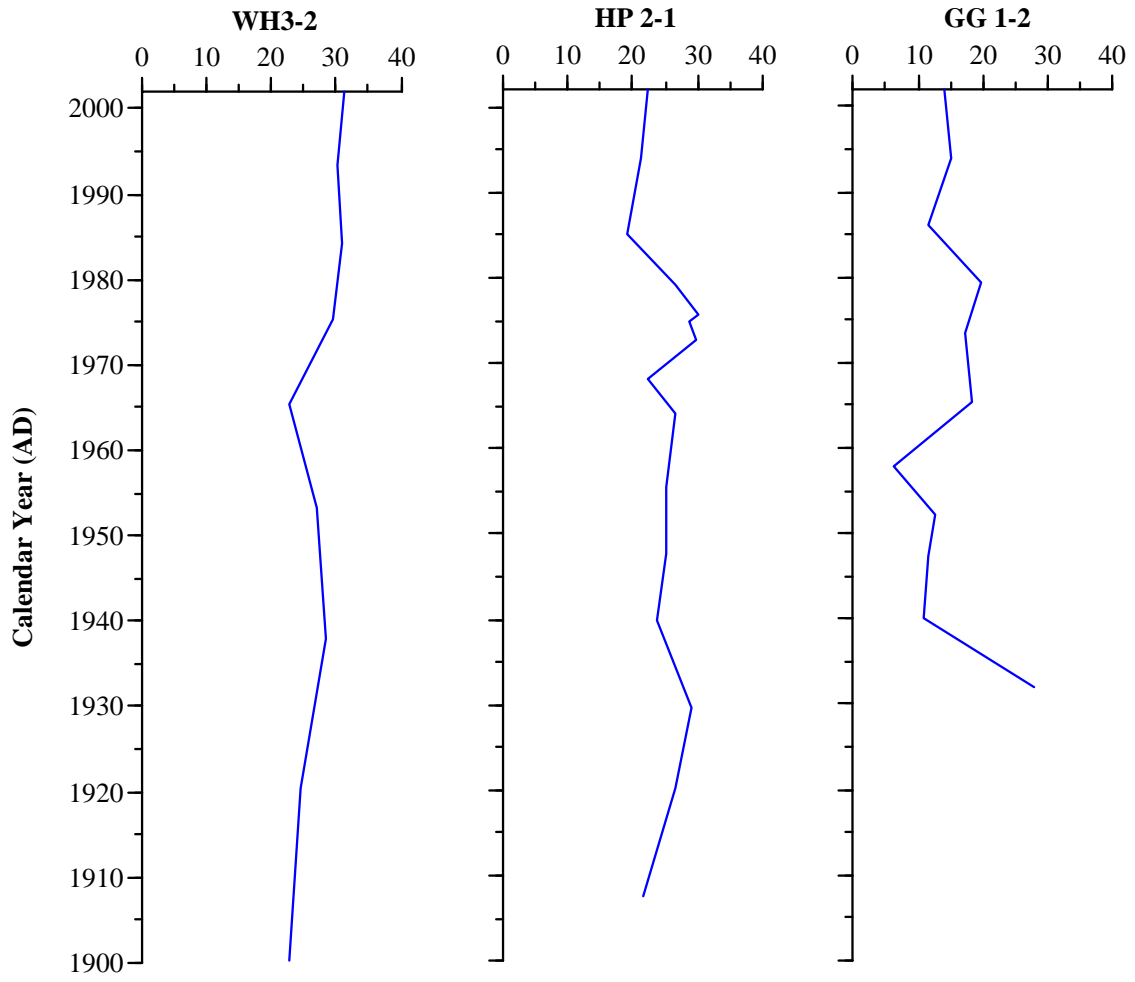


Figure 3.20. Percent organic carbon content from Watch Hill (WH 3-2), Hospital Point (HP 2-1) and Great Gun (GG 1-2) plotted versus calendar year AD.

Table 3.1 Fallout radionuclide concentrations in Fire Island core GG1-2

| Depth |                    | <sup>210</sup> Pb   |      |                     |      |                     |     | <sup>137</sup> Cs   |     | <sup>241</sup> Am   |     |
|-------|--------------------|---------------------|------|---------------------|------|---------------------|-----|---------------------|-----|---------------------|-----|
|       |                    | Total               |      | Unsupported         |      | Supported           |     |                     |     |                     |     |
| cm    | g cm <sup>-2</sup> | Bq kg <sup>-1</sup> | ±    | Bq kg <sup>-1</sup> | ±    | Bq kg <sup>-1</sup> | ±   | Bq kg <sup>-1</sup> | ±   | Bq kg <sup>-1</sup> | ±   |
| 0.5   | 0.1                | 218.6               | 13.6 | 202.2               | 13.8 | 16.3                | 2.3 | 5.7                 | 1.6 | 0.0                 | 0.0 |
| 2.5   | 0.8                | 187.7               | 13.1 | 167.3               | 13.3 | 20.4                | 2.7 | 8.0                 | 1.7 | 0.0                 | 0.0 |
| 4.5   | 1.5                | 90.0                | 7.9  | 73.4                | 8.1  | 16.6                | 1.8 | 5.4                 | 1.1 | 0.0                 | 0.0 |
| 6.5   | 2.2                | 107.3               | 10.9 | 87.4                | 11.2 | 20.0                | 2.7 | 10.6                | 1.9 | 0.0                 | 0.0 |
| 8.5   | 2.7                | 117.1               | 9.8  | 95.0                | 10.0 | 22.1                | 2.1 | 32.8                | 2.3 | 0.0                 | 0.0 |
| 10.5  | 3.2                | 131.4               | 9.0  | 110.2               | 9.3  | 21.2                | 2.1 | 98.7                | 2.5 | 4.0                 | 0.9 |
| 12.5  | 4.2                | 59.5                | 6.8  | 31.4                | 7.0  | 28.1                | 1.6 | 14.1                | 1.1 | 0.0                 | 0.0 |
| 14.5  | 5.3                | 57.8                | 7.7  | 37.9                | 7.9  | 19.9                | 1.8 | 26.6                | 1.6 | 0.0                 | 0.0 |
| 16.5  | 6.2                | 76.8                | 7.2  | 44.6                | 7.4  | 32.2                | 1.7 | 16.8                | 1.2 | 0.0                 | 0.0 |
| 18.5  | 7.0                | 73.9                | 9.1  | 50.6                | 9.2  | 23.2                | 1.4 | 3.2                 | 1.0 | 0.0                 | 0.0 |
| 20.5  | 7.6                | 93.9                | 7.4  | 69.3                | 7.6  | 24.6                | 1.7 | 2.2                 | 1.6 | 0.0                 | 0.0 |
| 22.5  | 8.0                | 51.6                | 9.1  | 37.5                | 9.3  | 14.1                | 2.0 | 0.0                 | 0.0 | 0.0                 | 0.0 |
| 24.5  | 8.4                | 16.2                | 7.9  | 4.2                 | 8.2  | 12.0                | 2.3 | 0.0                 | 0.0 | 0.0                 | 0.0 |
| 26.5  | 8.7                | 27.9                | 9.0  | 13.4                | 9.4  | 14.5                | 2.5 | 0.0                 | 0.0 | 0.0                 | 0.0 |
| 28.5  | 9.1                | 16.7                | 9.4  | -0.6                | 9.6  | 17.3                | 1.8 | 0.0                 | 0.0 | 0.0                 | 0.0 |
| 30.5  | 9.5                | 25.6                | 7.9  | 3.8                 | 8.2  | 21.8                | 2.3 | 0.0                 | 0.0 | 0.0                 | 0.0 |



Table 3.2 Fallout radionuclide concentrations in Fire Island core HP2-1

| Depth |                    | <sup>210</sup> Pb   |      |                     |      |                     |     | <sup>137</sup> Cs   |     |
|-------|--------------------|---------------------|------|---------------------|------|---------------------|-----|---------------------|-----|
| cm    | g cm <sup>-2</sup> | Total               |      | Unsupported         |      | Supported           |     | Bq kg <sup>-1</sup> | ±   |
|       |                    | Bq kg <sup>-1</sup> | ±    | Bq kg <sup>-1</sup> | ±    | Bq kg <sup>-1</sup> | ±   | Bq kg <sup>-1</sup> | ±   |
| 0.5   | 0.1                | 403.6               | 20.4 | 384.4               | 21.0 | 19.1                | 5.0 | 3.2                 | 2.9 |
| 2.5   | 0.4                | 322.2               | 17.9 | 294.3               | 18.5 | 27.9                | 4.7 | 6.6                 | 3.1 |
| 4.5   | 0.7                | 250.0               | 15.3 | 234.3               | 15.6 | 15.7                | 2.7 | 3.3                 | 2.6 |
| 6.5   | 1.0                | 134.3               | 15.2 | 100.9               | 15.8 | 33.3                | 4.5 | 2.0                 | 2.9 |
| 8.5   | 1.3                | 55.6                | 17.9 | 39.1                | 18.2 | 16.5                | 3.7 | 0.0                 | 0.0 |
| 10.5  | 1.6                | 38.9                | 19.2 | 12.9                | 19.5 | 26.0                | 3.6 | 0.6                 | 2.5 |
| 12.5  | 1.9                | 144.0               | 15.3 | 128.0               | 15.6 | 16.0                | 2.7 | 6.7                 | 2.2 |
| 14.5  | 2.2                | 80.1                | 13.9 | 54.6                | 14.3 | 25.5                | 3.4 | 20.3                | 3.4 |
| 16.5  | 2.6                | 76.3                | 9.6  | 60.8                | 9.8  | 15.5                | 2.2 | 82.7                | 3.2 |
| 18.5  | 2.9                | 64.5                | 13.1 | 49.8                | 13.7 | 14.7                | 3.9 | 28.4                | 2.9 |
| 20.5  | 3.2                | 40.9                | 9.8  | 18.3                | 10.3 | 22.6                | 3.2 | 44.5                | 2.7 |
| 22.5  | 3.6                | 70.3                | 10.7 | 40.2                | 11.2 | 30.2                | 3.1 | 20.3                | 2.4 |
| 24.5  | 3.9                | 39.7                | 12.0 | 19.1                | 12.2 | 20.6                | 2.3 | 9.2                 | 2.0 |
| 26.5  | 4.2                | 63.0                | 9.8  | 38.3                | 10.1 | 24.8                | 2.4 | 5.9                 | 2.2 |
| 28.5  | 4.5                | 48.1                | 8.1  | 27.4                | 8.4  | 20.7                | 2.1 | 7.9                 | 1.4 |
| 30.5  | 4.9                | 21.9                | 7.4  | -3.7                | 7.8  | 25.6                | 2.3 | 7.6                 | 1.6 |

Table 3.3 Fallout radionuclide concentrations in Fire Island core WH3-2

| Depth |                    | <sup>210</sup> Pb   |      |                     |      |                     |     | <sup>137</sup> Cs   |     | <sup>241</sup> Am   |     |
|-------|--------------------|---------------------|------|---------------------|------|---------------------|-----|---------------------|-----|---------------------|-----|
| cm    | g cm <sup>-2</sup> | Total               |      | Unsupported         |      | Supported           |     | Bq kg <sup>-1</sup> | ±   | Bq kg <sup>-1</sup> | ±   |
|       |                    | Bq kg <sup>-1</sup> | ±    | Bq kg <sup>-1</sup> | ±    | Bq kg <sup>-1</sup> | ±   | Bq kg <sup>-1</sup> | ±   | Bq kg <sup>-1</sup> | ±   |
| 0.5   | 0.1                | 496.1               | 36.3 | 485.2               | 36.8 | 10.9                | 5.9 | 0.0                 | 0.0 | 0.0                 | 0.0 |
| 2.5   | 0.5                | 492.5               | 20.8 | 472.0               | 21.3 | 20.5                | 4.4 | 3.4                 | 2.8 | 0.0                 | 0.0 |
| 4.5   | 0.9                | 308.8               | 14.9 | 292.3               | 15.2 | 16.5                | 2.9 | 4.3                 | 1.7 | 0.0                 | 0.0 |
| 6.5   | 1.3                | 246.7               | 18.8 | 241.6               | 19.2 | 5.1                 | 3.4 | 13.9                | 2.4 | 0.0                 | 0.0 |
| 8.5   | 1.8                | 214.1               | 12.7 | 185.7               | 13.1 | 28.4                | 3.2 | 128.3               | 3.8 | 7.3                 | 1.4 |
| 10.5  | 2.2                | 212.0               | 15.6 | 192.6               | 16.0 | 19.4                | 3.4 | 20.5                | 3.0 | 0.0                 | 0.0 |
| 12.5  | 2.5                | 143.0               | 14.9 | 123.0               | 15.1 | 20.0                | 2.8 | 4.2                 | 1.9 | 0.0                 | 0.0 |
| 14.5  | 2.9                | 41.9                | 16.3 | 26.9                | 16.6 | 15.0                | 2.7 | 0.0                 | 0.0 | 0.0                 | 0.0 |
| 16.5  | 3.4                | 54.4                | 6.4  | 25.9                | 6.6  | 28.5                | 1.7 | 0.0                 | 0.0 | 0.0                 | 0.0 |
| 18.5  | 3.9                | 16.2                | 3.8  | 2.2                 | 4.6  | 14.0                | 2.5 | 0.0                 | 0.0 | 0.0                 | 0.0 |
| 20.5  | 4.3                | 15.9                | 8.9  | -2.8                | 9.1  | 18.6                | 2.0 | 0.9                 | 1.8 | 0.0                 | 0.0 |

Table 3.4 Radionuclide parameters for Fire Island cores

| Core             | Unsupported $^{210}\text{Pb}$ |    |                    |     |                                    | $^{137}\text{Cs}$ |                    |    |
|------------------|-------------------------------|----|--------------------|-----|------------------------------------|-------------------|--------------------|----|
|                  | Maximum activity              |    | Inventory          |     | Flux                               | Inventory         |                    |    |
|                  | Bq kg <sup>-1</sup>           | ±  | Bq m <sup>-2</sup> | ±   | Bq m <sup>-2</sup> y <sup>-1</sup> | ±                 | Bq m <sup>-2</sup> | ±  |
| Fire Island      |                               |    |                    |     |                                    |                   |                    |    |
| GG1-2            | 202                           | 14 | 6221               | 250 | 194                                | 8                 | 1664               | 52 |
| HP2-1            | 384                           | 21 | 4355               | 191 | 136                                | 6                 | 809                | 35 |
| WH3-2            | 485                           | 37 | 7732               | 258 | 241                                | 8                 | 739                | 35 |
| Mean values      | 357                           |    | 6103               |     | 190                                |                   | 1071               |    |
| Atmospheric flux |                               |    |                    |     | 154                                |                   | 3028               |    |

Table 3.5  $^{210}\text{Pb}$  chronology of Fire Island core GG1-2. In italics, chronology for pre-1920 sediments (below 22 cm) is highly uncertain.

| Depth |                    | Chronology  |           |           | Sedimentation Rate                 |                    |       |
|-------|--------------------|-------------|-----------|-----------|------------------------------------|--------------------|-------|
| cm    | g cm <sup>-1</sup> | Date AD     | Age y     | ±         | g cm <sup>-2</sup> y <sup>-1</sup> | cm y <sup>-1</sup> | ± (%) |
| 0.0   | 0.0                | 2002        | 0         | 0         |                                    |                    |       |
| 0.5   | 0.1                | 2000        | 2         | 1         | 0.079                              | 0.25               | 11.2  |
| 2.5   | 0.8                | 1992        | 10        | 2         | 0.074                              | 0.25               | 13.7  |
| 4.5   | 1.5                | 1984        | 18        | 3         | 0.133                              | 0.29               | 17.8  |
| 6.5   | 2.2                | 1978        | 24        | 3         | 0.092                              | 0.32               | 21.0  |
| 8.5   | 2.7                | 1972        | 30        | 4         | 0.069                              | 0.26               | 22.7  |
| 10.5  | 3.2                | 1963        | 39        | 5         | 0.078                              | 0.26               | 29.1  |
| 12.5  | 4.2                | 1956        | 46        | 6         | 0.193                              | 0.34               | 37.1  |
| 14.5  | 5.3                | 1951        | 51        | 8         | 0.141                              | 0.37               | 46.0  |
| 16.5  | 6.2                | 1946        | 56        | 9         | 0.118                              | 0.31               | 19.4  |
| 18.5  | 7.0                | 1938        | 64        | 11        | 0.080                              | 0.26               | 23.4  |
| 20.5  | 7.6                | 1930        | 72        | 12        | 0.040                              | 0.18               | 33.5  |
| 22.5  | 8.0                | <i>1915</i> | <i>87</i> | <i>14</i> | <i>0.039</i>                       | <i>0.20</i>        |       |
| 24.5  | 8.4                | <i>1910</i> | <i>92</i> | <i>15</i> | <i>0.086</i>                       | <i>0.46</i>        |       |
| 26.5  | 8.7                | <i>1907</i> | <i>95</i> | <i>17</i> | <i>0.122</i>                       | <i>0.61</i>        |       |

Table 3.6 <sup>210</sup>Pb chronology of Fire Island core HP2-1

| Depth |                    | Chronology |          |    | Sedimentation Rate                 |                    |       |
|-------|--------------------|------------|----------|----|------------------------------------|--------------------|-------|
| cm    | g cm <sup>-1</sup> | Date<br>AD | Age<br>y | ±  | g cm <sup>-2</sup> y <sup>-1</sup> | cm y <sup>-1</sup> | ± (%) |
| 0.0   | 0.0                | 2002       | 0        | 0  |                                    |                    |       |
| 0.5   | 0.1                | 2000       | 2        | 1  | 0.037                              | 0.25               | 8.2   |
| 2.5   | 0.4                | 1992       | 10       | 2  | 0.041                              | 0.24               | 9.8   |
| 4.5   | 0.7                | 1983       | 19       | 2  | 0.040                              | 0.28               | 11.7  |
| 6.5   | 1.0                | 1978       | 24       | 3  | 0.067                              | 0.51               | 19.3  |
| 8.5   | 1.3                | 1975       | 27       | 3  | 0.147                              | 1.25               | 48.1  |
| 10.5  | 1.6                | 1975       | 27       | 3  | 0.341                              | 1.18               | 59.1  |
| 12.5  | 1.9                | 1972       | 30       | 3  | 0.050                              | 0.52               | 17.5  |
| 14.5  | 2.2                | 1967       | 35       | 4  | 0.076                              | 0.44               | 29.9  |
| 16.5  | 2.6                | 1963       | 39       | 4  | 0.053                              | 0.30               | 22.9  |
| 18.5  | 2.9                | 1953       | 49       | 7  | 0.039                              | 0.24               | 31.5  |
| 20.5  | 3.2                | 1946       | 56       | 9  | 0.043                              | 0.26               | 58.5  |
| 22.5  | 3.6                | 1938       | 64       | 12 | 0.034                              | 0.21               | 33.8  |
| 24.5  | 3.9                | 1927       | 75       | 14 | 0.032                              | 0.20               | 66.9  |
| 26.5  | 4.2                | 1918       | 84       | 17 | 0.027                              | 0.17               |       |
| 28.5  | 4.5                | 1904       | 98       | 19 | 0.031                              | 0.17               |       |

Table 3.7 <sup>210</sup>Pb chronology of Fire Island core WH3-2

| Depth |                    | Chronology |          |    | Sedimentation Rate                 |                    |       |
|-------|--------------------|------------|----------|----|------------------------------------|--------------------|-------|
| cm    | g cm <sup>-1</sup> | Date<br>AD | Age<br>y | ±  | g cm <sup>-2</sup> y <sup>-1</sup> | cm y <sup>-1</sup> | ± (%) |
| 0.00  | 0.00               | 2002       | 0        | 0  |                                    |                    |       |
| 0.50  | 0.11               | 2000       | 2        | 1  | 0.051                              | 0.23               | 13.2  |
| 2.50  | 0.51               | 1991       | 11       | 2  | 0.040                              | 0.22               | 14.8  |
| 4.50  | 0.90               | 1982       | 20       | 3  | 0.049                              | 0.22               | 19.2  |
| 6.50  | 1.31               | 1973       | 29       | 5  | 0.045                              | 0.21               | 25.5  |
| 8.50  | 1.76               | 1963       | 39       | 8  | 0.042                              | 0.18               | 34.0  |
| 10.50 | 2.17               | 1950       | 52       | 9  | 0.022                              | 0.14               | 39.6  |
| 12.50 | 2.53               | 1934       | 68       | 15 | 0.022                              | 0.12               | 39.6  |
| 14.50 | 2.92               | 1916       | 86       | 24 | 0.022                              | 0.10               | 39.6  |
| 16.50 | 3.39               | 1895       | 107      | 36 | 0.022                              | 0.09               | 39.6  |

Table 3.8 Mean post-1963 sedimentation rates in Fire Island cores

| Core        | Sedimentation rate               |                    |
|-------------|----------------------------------|--------------------|
|             | $\text{g cm}^{-2} \text{y}^{-1}$ | $\text{cm y}^{-1}$ |
| Fire Island |                                  |                    |
| GG1-2       | 0.082                            | 0.27               |
| HP2-1       | 0.066                            | 0.42               |
| WH302       | 0.045                            | 0.22               |
| Mean value  | 0.064                            | 0.30               |

Table 3.9. Comparison of marsh accretion rates using three methods.

| Location       | Feldspar Horizon<br>Accretion<br>( $\text{mm yr}^{-1}$ ) | Recent $^{210}\text{Pb}$ 2002 - 2000 AD<br>( $\text{mm yr}^{-1}$ ) | Post 1963 average $^{137}\text{Cs}$<br>( $\text{mm yr}^{-1}$ ) |
|----------------|--|--|--|
| Great Gun      | 2.12   | 2.50   | 2.70   |
| Hospital Point | 3.76   | 2.50   | 4.20   |
| Watch Hill     | 3.67   | 2.30   | 2.20   |

## CHAPTER 4

### Summary of Findings and Management Implications

Contributing Authors: Charles T. Roman, John W. King, Donald R. Cahoon

---

#### PURPOSE AND SIGNIFICANCE OF THE STUDY

Salt marshes are dynamic environments, increasing in vertical elevation and migrating, often landward, as sea level rises (Redfield 1965, Donnelly and Bertness 2001). With sea level rise greater than marsh elevation increase, marshes can be submerged, marsh soils become waterlogged, and plant growth becomes stressed, often resulting in conversion of vegetation-dominated marsh to mudflat or open water habitat (e.g., Orson et al. 1985). Given that the rate of sea level rise is expected to accelerate over the next century (Gornitz 1995, Meehl et al. 2007) and that some marshes in the northeast are becoming submerged (e.g., Jamaica Bay, NY, Hartig et al. 2002), it is important to understand the processes that control marsh development. More specifically, the objectives of this project were to quantify vertical marsh elevation change in relation to recent rates of sea-level rise and to investigate factors or processes that are most influential in controlling the development and maintenance of Fire Island salt marshes.

#### STUDY SITE AND METHODS: A REVIEW

The 50-km Fire Island is located on the south shore of Long Island (NY). The island is bordered by Moriches Inlet to the east and Fire Island Inlet to the west, exchanging with the Atlantic Ocean and the back-barrier lagoon system of Great South Bay and Moriches Bay. *Spartina alterniflora* dominated salt marsh occurs along the bay shoreline of Fire Island, with the greatest area of marshes within the eastern portion of the island. Mean tidal range of the back-barrier lagoon tends to be greater near the inlets (60-70 cm) and much reduced at locations remote from the inlets (18-20 cm). To reflect this gradient of tidal range and proximity to existing inlets and to represent the diversity of physical conditions that may influence salt marsh development at Fire Island, three study marshes were selected; Great Gun Meadows, Hospital Point, and Watch Hill, 2.5 km, 12 km, and 20 km, respectively, from Moriches Inlet (see Fig. 1.1).

Surface Elevation Tables (SETs), in conjunction with feldspar marker horizons, were used to evaluate recent (2002 to 2007) relationships between marsh surface elevation change and rates of relative sea level rise and understand the surface and subsurface processes that influence marsh elevation change. The elevation of a salt marsh is controlled by sediment accretion and organic matter build-up, resulting in increases in elevation, while the subsurface processes of sediment compaction/subsidence and organic

matter decomposition, as well as erosion of surface sediments contribute to elevation loss. The surface accretionary processes are monitored by repeated sampling of artificial marker horizon plots and marsh surface elevation is correspondingly monitored with the surface elevation table. This method enables an interpretation of how surface processes (deposition and erosion) and subsurface processes (compaction, decomposition, organic matter accumulation) influence marsh elevation. SETs and marker horizons were established at the three marsh areas in August 2002, with monitoring proceeding at 3-4 month intervals during the spring-to-fall period (see Fig. 2.1). Data reported in this report are for the 58 month period from August 2002 to May 2007. SET and marker horizon monitoring is planned to continue for the long-term. Marsh surface elevation change is compared to sea level rise to determine if the marsh is keeping pace with sea level or becoming submerged.

To evaluate longer-term or historic trends (decades to centuries) in marsh development processes at Fire Island, sediment cores approximately 1-m deep, were collected from the three marsh areas. Stratigraphy of the cores was evaluated by digital imagery and measures of magnetic susceptibility, wet bulk density, and organic content by loss-on-ignition. Radiometric dating of the cores was accomplished by  $^{210}\text{Pb}$  and  $^{137}\text{Cs}$ .

## **FINDINGS: RECENT TRENDS IN MARSH DEVELOPMENT PROCESSES**

All three sites reveal an elevation deficit when compared to sea level rise; the marshes appear to not be keeping pace with recent rates of sea level rise (see Fig. 2.3). Based on the SET elevation monitoring during the 58 month study period, elevation change of the marsh surface ranged from an increase of  $2.04 \text{ mm y}^{-1}$  and  $2.08 \text{ mm y}^{-1}$  at Hospital Point and Watch Hill, respectively, to an elevation decline of  $-1.05 \text{ mm y}^{-1}$  at Great Gun. Long-term records of relative sea level from NOAA water level stations in the vicinity of Great South Bay/Moriches Bay (Montauk Point and Battery, NY; Sandy Hook, NJ) ranged from  $2.52 \text{ mm y}^{-1}$  to  $3.79 \text{ mm y}^{-1}$ , all greater than measured marsh elevation changes.

At each site vertical accretion (measured by the feldspar marker horizons) was greater than the marsh surface elevation change at all sites. Sediment accumulated on the marsh surface (vertical accretion), but the elevation of the marsh surface did not reflect this accumulation, suggesting shallow subsidence (surface accretion is greater than elevation gain). Shallow subsidence is a fairly common occurrence (Cahoon et al. 1999), and suggests that subsurface processes such as autocompaction of marsh sediments, decomposition of belowground organic matter, and changes in belowground water storage are likely all contributing to the observed elevation deficit.

It is noted that the SET and horizon marker monitoring reported in this paper encompasses a relative short time-period that may not be fully adequate to integrate the complexity of processes that control marsh surface elevation dynamics. For instance, during the study period there were no major storm events, a principle mechanism for the delivery of sediments to the marsh surface.

## **FINDINGS: HISTORIC TRENDS, THE ROLE OF INLETS IN MARSH DEVELOPMENT**

Based on the chronology from radiometric dating of the cores, it was estimated that salt marsh development was initiated at the Great Gun site around 1766 AD and Hospital Point near 1778. Given the errors associated with extrapolating the core chronologies, it is noted that at both sites salt marsh initiation appears to coincide with establishment of nearby Halletts (1788) and Smiths (1773) inlets, respectively. The role of storm-induced inlets and barrier island overwash events in the bayward transport of sediment, flood tidal delta formation, and marsh development is well-known (e.g., Leatherman 1979, Fisher and Simpson 1979, Donnelly et al. 2004). Salt marsh initiation at the Watch Hill site was estimated at 1589 AD; records of inlet formation prior to the Colonial period were not found, but it is expected that initiation of this marsh area was also in response to an inlet or major overwash event. Also related to inlets, at the Great Gun marsh there was a clear correlation between the opening of Moriches Inlet in 1931 and the abrupt termination of salt marsh peat development, replaced by deposition of inorganic sediment. It is likely that the tidal range increased substantially at Great Gun with the opening of the new inlet, the existing *Spartina* marsh was inundated and converted to tidal flat, then with subsequent re-development of marsh to the present as hydrologic conditions became favourable for vegetation to thrive.

## **RESOURCE MANAGEMENT IMPLICATIONS AND RESEARCH NEEDS**

It is clear from this study, and the literature, that inlets and associated flood tidal deltas represent a fundamental process supporting the establishment of back-barrier salt marsh habitat. The long-term maintenance of salt marshes at Fire Island seems tightly coupled to preservation of inlet processes.

Recent trends in marsh surface elevation suggest that the Fire Island marshes are not keeping pace with sea level rise. If the observed elevation deficit continues, it is likely that the Fire Island marshes will become wetter, areas of high marsh *Spartina patens* may convert to *Spartina alterniflora* (as noted in a southern New England marsh, Donnelly and Bertness 2001), and open water habitat may increase. There could also be a landward encroachment of marshes to upland areas, a natural process of marsh development in response to sea level rise (Redfield 1965), assuming that cultural development (e.g., bulkheads) will not impede this migration.

Salt marsh elevation monitoring, coupled with vegetation and marsh landscape change analysis, will continue for the long-term in association with the National Park Service Northeast Coastal and Barrier Monitoring Network, enabling a better understanding of relationships between marsh development processes and habitat responses.

The long-term maintenance of salt marshes at Fire Island is dependent, in part, on geomorphic processes of sediment delivery to the marshes. Research is necessary to

quantify suspended sediment concentrations and volume transport mechanisms to the marsh surface, especially during storm events. It is also important to understand the effects of shoreline stabilization efforts and channel dredging on sediment transport processes to marshes. Further, research is needed to better understand the role of shallow subsurface processes in the observed marsh elevation deficit at Fire Island marshes.

## LITERATURE CITED

Cahoon, D.R., J.W. Day, Jr., and D.J. Reed. 1999. The influence of surface and shallow subsurface soil processes on wetland elevation: a synthesis. *Current Topics in Wetland Biogeochemistry* 3: 72-88.

Donnelly, J.P., and M.D. Bertness. 2001. Rapid shoreward encroachment of salt marsh cordgrass in response to accelerated sea-level rise. *Proceedings of the National Academy of Sciences* 98: 14218-14223.

Donnelly, J.P., J. Butler, S. Roll, M. Wengren, and T. Webb III. 2004. A backbarrier overwash record of intense storms from Brigantine, New Jersey. *Marine Geology* 107-121.

Fisher, J.J., and E. J. Simpson. 1979. Washover and tidal sedimentation rates as environmental factors in development of a transgressive barrier shoreline. Pages 127 – 148 in *Barrier Islands from the Gulf of St. Lawrence to the Gulf of Mexico* (S.P. Leatherman, ed.). Academic Press, NY.

Gornitz, V. 1995. Sea-level rise: a review of recent, past and near-future trends. *Earth Surface Processes and Landforms* 20: 7-20.

Hartig, E.K., V. Gronitz, A. Kolker, F. Muchacke, and D. Fallon. 2002. Anthropogenic and climate-change impacts on salt marshes of Jamaica Bay, New York City. *Wetlands* 22: 71-89.

Leatherman, S.P. 1979. Migration of Assateague Island, Maryland, by inlet and overwash processes. *Geology* 7: 104-107.

Meehl, G.A., T.F. Stocker, W.D. Collins, P. Friedlingstein, A.T. Gaye, .M. Gregory, A. Kitoh, R. Knutti, J.M. Murphy, A. Noda, S.C.B. Raper, I.G. Watterson, A.J. Weaver, and Z.C. Zhao. 2007. Global Climate Projections, Chapter 10. Pages 747-822 in *Climate Change 2007: The Physical Science Basis. Contribution of Working Group I to the Fourth Assessment Report of the Intergovernmental Panel on Climate Change* (Solomon, S., D. Qin, M. Manning, Z. Chen, M. Marquis, K.I.B. Averyt, M. Tignor and H.L. Miller, editors). Cambridge University Press, Cambridge, United Kingdom and New York, NY.

Redfield, A.C. 1965. Ontogeny of a salt marsh estuary. *Science* 147: 50-55.



As the nation's primary conservation agency, the Department of the Interior has responsibility for most of our nationally owned public land and natural resources. This includes fostering sound use of our land and water resources; protecting our fish, wildlife, and biological diversity; preserving the environmental and cultural values of our national parks and historical places; and providing for the enjoyment of life through outdoor recreation. The department assesses our energy and mineral resources and works to ensure that their development is in the best interests of all our people by encouraging stewardship and citizen participation in their care. The department also has a major responsibility for American Indian reservation communities and for people who live in island territories under U.S. administration.

**National Park Service**  
**U.S. Department of the Interior**



---

**Northeast Region**  
Natural Resource Stewardship and Science  
15 State Street  
Boston, Massachusetts 02109

<http://www.nps.gov/nero/science/>

**EXPERIENCE YOUR AMERICA™**